

Implications of the measurements of $B_s-\overline{B}_s$ mixing on SUSY models

P. Ko

School of Physics, KIAS, Seoul 130-722, Korea

E-mail: pko@kias.re.kr

Jae-hyeon Park

INFN, Sezione di Padova, via F Marzolo 8, I-35131, Padova, Italy

E-mail: jae-hyeon.park@pd.infn.it

ABSTRACT: We derive constraints on the mass insertion parameters from the recent measurements of $B_s-\overline{B}_s$ mixing, and discuss their implications on SUSY breaking mediation mechanisms and SUSY flavor models. Some SUSY flavor models are already excluded or disfavored by $B_s-\overline{B}_s$ mixing. We also discuss how to test the SM and SUSY models in the future experiments, by studying other CP violating observables related to $b \rightarrow s$ transition, such as the time-dependent CP asymmetry in $B_d \rightarrow \phi K_S$ and the direct CP asymmetry in $B \rightarrow X_s \gamma$.

Contents

1. Introduction	1
2. Models and analysis procedures	3
2.1 Gluino-mediated flavor violation and mass insertion approximation	3
2.2 $\Delta B = 2$ effective Hamiltonian	5
2.3 $\Delta B = 1$ effective Hamiltonian	6
2.4 New elements in this analysis	9
2.5 Double mass insertion	10
2.6 Numerical analysis	11
3. SUSY effects in $b \rightarrow s$ after the CDF/DØ measurements of ΔM_s	12
3.1 LL insertion case	12
3.2 RR insertion case	12
3.3 $LL = RR$ case	15
3.4 $LL = -RR$ case	17
3.5 Implications for $B_s \rightarrow \mu^+ \mu^-$	19
4. Implications for SUSY models	21
4.1 SUSY models with universal scalar masses	21
4.2 SUSY flavor models	22
5. Conclusions	23

1. Introduction

Within the Standard Model (SM) with three families, there is a unique source of flavor and CP violation in the quark sector, which is the renowned Cabbibo-Kobayashi-Maskawa (CKM) mixing matrix [1]. The CKM paradigm has long been tested in the K , D and B meson systems during the last decades. As of now, this picture has been well confirmed to describe basically all the data related with flavor and CP violation in the quark sector, modulo some theoretical and experimental uncertainties. Experimental uncertainties will be decreased as more data are taken at B factories, whereas theoretical uncertainties will be under better control when more results come from unquenched lattice QCD simulations on various nonperturbative parameters that are relevant to CKM analysis.

For many years, one of the important ingredients in the CKM phenomenology was still missing, namely ΔM_s from B_s - \bar{B}_s mixing. Recently, however, ΔM_s was measured by both DØ and CDF Collaborations at the Tevatron:

$$17 \text{ ps}^{-1} < \Delta M_s < 21 \text{ ps}^{-1} \quad (\text{DØ}) [2], \quad (1.1)$$

$$\Delta M_s = (17.77 \pm 0.10 \pm 0.07) \text{ ps}^{-1} \quad (\text{CDF}) \quad [3]. \quad (1.2)$$

One can use the measured value of $\Delta M_d/\Delta M_s$ to determine $|V_{td}/V_{ts}|$ within the SM [3]:

$$|V_{td}/V_{ts}| = 0.2060 \pm 0.0007 (\Delta M_s)_{-0.0060}^{+0.0081} (\Delta M_d + \text{theor}). \quad (1.3)$$

This result is consistent with another independent determination of $|V_{td}/V_{ts}|$ from the Belle measurement of a radiative decay $B \rightarrow X_d \gamma$ [4]:

$$|V_{td}/V_{ts}| = 0.199_{-0.025}^{+0.026}(\text{exp})_{-0.015}^{+0.018}(\text{theor}). \quad (1.4)$$

Excellent agreement of these two independent measurements constitutes another firm test of the CKM paradigm for flavor and CP violation in the SM [5, 6], and puts strong constraints on various new physics scenarios. There are model independent analyses of ΔM_s measurements on general new physics [7, 8], as well as analyses within supersymmetric (SUSY) models [9, 10] and others [11]. Due to these data on ΔM_s , the CKM paradigm is more constrained than before, and there may be even a slight hint for new physics beyond the SM (see Ref. [8], for example).

Within the SM, $B_s-\overline{B}_s$ mixing is dominated by t - W loop, and the $B_s-\overline{B}_s$ mixing phase is suppressed by λ^2 [12]. Due to its small theoretical uncertainty, observation of a nonzero discrepancy in the phase of $B_s-\overline{B}_s$ mixing would be an unambiguous signal of new physics beyond the SM in $b \rightarrow s$ transition [13]. Such new physics effects, if any, may appear in other observables in the $B_{(d,s)}$ meson systems, e.g., $B_d \rightarrow \phi K_S$ or $B \rightarrow X_s \gamma$.

The two collaborations also reported results on the phase of $B_s - \overline{B}_s$ mixing from the time dependent CP asymmetry in $B_s \rightarrow J/\psi \phi$ and the charge asymmetry (or CP violation in the mixing) in the B_s system:

$$A_{\text{SL}} \equiv \frac{N(B_s B_s) - N(\overline{B}_s \overline{B}_s)}{N(B_s B_s) + N(\overline{B}_s \overline{B}_s)} \approx \text{Im} \left(\frac{\Gamma_{12} \approx \Gamma_{12}^{\text{SM}}}{M_{12}^{\text{SM}} + M_{12}^{\text{SUSY}}} \right). \quad (1.5)$$

The results are

$$\phi_s = -0.57_{-0.30}^{+0.24}(\text{stat})_{-0.02}^{+0.07}(\text{syst}) \quad (\text{D}\mathcal{O}) \quad [14], \quad (1.6)$$

$$\phi_s \in [-1.36, -0.24] \cup [-2.90, -1.78] \quad (\text{CDF}) \quad [15], \quad (1.7)$$

at 68% CL. These measurements give a strong constraint on the new physics contributions to $B_s-\overline{B}_s$ mixing, both the modulus and the phase of the mixing. In general SUSY models, this will constrain the 23 mixing, $(\delta_{23}^d)_{AB}$ with $A, B = L$ or R .

In this paper, we update our previous studies on $b \rightarrow s$ transitions within the general SUSY models [16, 17] using the new data on B_s mixing from D \mathcal{O} and CDF, and discuss their implications for SUSY models. In Sec. 2, we describe the general SUSY models with gluino-mediated flavor/CP violation in brief, and how to proceed and analyze the SUSY models. Compared with the previous studies, we consider the $\tan \beta$ dependent constraint carefully including the double mass insertions, which can be prominent in $B \rightarrow X_s \gamma$ for large $\tan \beta$. In Sec. 3, we present the constraints on the mass insertion parameters for several different scenarios: the LL or the RR dominance case, and $LL = \pm RR$ cases.

We also mention briefly the implications of our results on $B_s \rightarrow \mu^+ \mu^-$, which can give important informations on δ 's in the large $\tan \beta$ region. In Sec. 4, we discuss implications of the newly derived bounds on the mass insertion parameters on SUSY models. Most SUSY models with universal soft scalar masses at some high energy scale or many SUSY models with flavor symmetry groups are still consistent with our new constraints. But some SUSY flavor models based on flavor symmetries and alignment of quark and squark mass matrices are shown to be in conflict with our constraints, and thus excluded or disfavored, depending on $\tan \beta$. In Sec. 5, we summarize our results and discuss the prospects in the future directions in theory and experiments which should be taken in order to test the CKM paradigm and see by any chance some new physics effects lurking in $b \rightarrow s$ transitions.

2. Models and analysis procedures

2.1 Gluino-mediated flavor violation and mass insertion approximation

The minimal supersymmetric standard model (MSSM) has many nice motivations such as resolution of fine tuning problem of Higgs mass parameter, gauge coupling unification, and cold dark matter [18]. But SUSY, if it exists, must be broken, and SUSY breaking effect is described phenomenologically by more than 100 new parameters in the so-called soft SUSY breaking lagrangian. These soft SUSY breaking parameters generically violate both flavor and CP. If these parameters take generic values, one ends up with excessive flavor and CP violations which are already inconsistent with such low energy data as $K^0-\bar{K}^0$ mixing, ϵ_K , $B \rightarrow X_s \gamma$ and electron/neutron electric dipole moments (EDMs). Therefore, there must be some mechanism which controls the structures of flavor changing neutral currents (FCNCs) and CP in the soft SUSY breaking terms, if weak scale SUSY has anything to do with Nature. This may be achieved by means of the SUSY breaking mediation mechanism which is flavor blind, and/or some flavor symmetry controlling both Yukawa couplings and sfermion mass matrices in flavor space. In a different point of view, we could get a clue to these SUSY breaking mediation mechanisms by studying FCNC and CP in supersymmetric models.

In SUSY models, there are new contributions to $B_s-\bar{B}_s$ mixing from H^-t , $\chi^--\tilde{U}_i$ and $\tilde{D}_i-\tilde{g}(\tilde{\chi}^0)$ in addition to the SM t - W loop. In generic SUSY models, the squark-gluino loop contribution is parametrically larger than other contributions, since it is strong interaction. In this work, we assume that the dominant SUSY contribution to B_s mixing comes from down squark-gluino loop diagrams. This assumption simplifies the numerical analysis considerably. Including effects from other SUSY particles is straightforward, and similar analysis could be done. A similar analysis for the $b \rightarrow d$ transition has been performed within the mass insertion approximation [19], using $B_d-\bar{B}_d$ mixing, A_{SL}^d and CP violation in $B \rightarrow X_d \gamma$ under the same assumptions.

Mass insertion approximation is a useful tool to present flavor and CP violations in the sfermion sector in generic SUSY models [20]. The parameter $(\delta_{ij}^d)_{AB}$ represents the dimensionless transition strength from \tilde{d}_{jB} to \tilde{d}_{iA} in the basis where the fermion Yukawa couplings are diagonal (SCKM basis), where $i, j = 1, 2, 3$ are generation indices and $A, B =$

L, R are chiralities of superpartners of quarks¹. If $(\delta_{ij}^d)_{AB} \sim O(1)$, there are excessive FCNC and CP violations with strong interaction couplings, which are clearly excluded by the data. Therefore δ 's should be small, $\lesssim 10^{-1}-10^{-3}$ with upper bounds depending on (i, j, A, B) , which is so called the SUSY FCNC/CP problem.

Current global analysis of the CKM matrix elements indicates that any new physics around TeV scale should be flavor/CP blind to a very good approximation. Therefore it would be nice if we can set $\delta = 0$. However, even if we set δ 's to zero by hand at one energy scale (presumably at high energy scale), nonzero δ 's are regenerated at electroweak scale due to the renormalization group (RG) evolution, and we cannot make δ 's vanish at all scales. It is most likely that δ 's are nonvanishing at electroweak scale. Then, the relevant questions are how large or small δ parameters are in a given SUSY breaking scenario, and what are the observable consequences of nonzero δ 's in flavor and CP violation beyond the effects derived from CKM matrix elements. These issues will be addressed in the subsequent sections.

Since flavor physics and CP violation such as $B \rightarrow X_s \gamma$, $B_s \rightarrow \mu^+ \mu^-$, ϵ_K within SUSY models depend strongly on soft SUSY breaking sector which is not well understood yet, it is important not to make an *ad hoc* assumption on the soft terms. For example, the usual assumption in the mSUGRA scenario is not well motivated theoretically, although it seems acceptable phenomenologically since it solves the SUSY flavor and CP problem. However such assumptions are made for the sake of simplicity in studying flavor physics, dark matter and collider physics signatures within SUSY context. Sometimes, it gives wrong intuitions, some examples of which can be found in Ref.s [21].

In the following, we at first consider δ 's as free parameters at the electroweak scale, and derive phenomenological constraints on these parameters, including $B \rightarrow X_s \gamma$ and the newly measured $B_s-\bar{B}_s$ mixing. Then we estimate the δ 's in various SUSY breaking scenarios, and investigate which models pass the phenomenological constraints on δ parameters. We assume δ 's vanish at some scale (messenger scale), where soft SUSY breaking terms are generated, and study the size of the δ 's that are generated by RG evolutions down to the electroweak scale. Alternatively, we consider SUSY flavor models where δ 's are controlled by some flavor symmetry group that acts on the flavor indices of quarks and their superpartners.

In terms of mass insertion parameters $(\delta_{ij}^d)_{AB}$, the down-type squark mass matrix of second and third families can be written as

$$M_d^2 = \begin{pmatrix} \tilde{m}_L^2 + \tilde{m}^2 & \tilde{m}^2 (\delta_{23}^d)_{LL} & m_s(A_s - \mu \tan\beta) & \tilde{m}^2 (\delta_{23}^d)_{LR} \\ \tilde{m}^2 (\delta_{23}^d)_{LL}^* & \tilde{m}_L^2 + \tilde{m}^2 & \tilde{m}^2 (\delta_{23}^d)_{RL}^* & m_b(A_b - \mu \tan\beta) \\ m_s(A_s - \mu \tan\beta) & \tilde{m}^2 (\delta_{23}^d)_{RL} & \tilde{m}_R^2 + \tilde{m}^2 & \tilde{m}^2 (\delta_{23}^d)_{RR} \\ \tilde{m}^2 (\delta_{23}^d)_{LR}^* & m_b(A_b - \mu \tan\beta) & \tilde{m}^2 (\delta_{23}^d)_{RR}^* & \tilde{m}_R^2 + \tilde{m}^2 \end{pmatrix}, \quad (2.1)$$

where \tilde{m}^2 is the universal part of soft SUSY breaking scalar mass squared, and

$$\begin{aligned} \tilde{m}_L^2 &= -\frac{1}{6} \cos 2\beta (m_Z^2 + 2m_W^2), \\ \tilde{m}_R^2 &= -\frac{1}{3} \cos 2\beta (m_Z^2 - m_W^2), \end{aligned} \quad (2.2)$$

¹A quantitative definition of the δ parameters will be given below.

are D -term contributions. We neglect $m_{\tilde{d}}^2$ terms. We assume that A -terms are negligible, and the μ parameter is real. Relaxing the former assumption is straightforward, and would not change the results significantly. The latter assumption is made to satisfy EDM constraints. By using mass insertion parameters, we have implicitly specified the basis of squark flavors, i.e. the above matrix is in the super CKM basis. The unitary matrix U diagonalizing the mass matrix is divided into two parts, Γ_L and Γ_R , according to the quark chirality to which they are associated, as

$$\begin{aligned} M_{\tilde{d}}^2 &= U^\dagger M_{\tilde{d}}^{2(\text{diag})} U, \\ \Gamma_L^{Ij} &\equiv U_j^I, \\ \Gamma_R^{Ij} &\equiv -U_{j+3}^I, \end{aligned} \tag{2.3}$$

where $M_{\tilde{d}}^{2(\text{diag})}$ is a diagonal matrix with positive elements, $I = 1, \dots, 6$ is the squark mass eigenstate index, and $j = 1, 2, 3$ is the quark mass eigenstate index. Note that we absorb the relative minus sign between quark-squark-gluino vertices of opposite chiralities into that in the definition of Γ_R^{Ij} . We give a name r_I to the ratio of a squark squared mass eigenvalue to the gluino mass squared,

$$r_I \equiv \frac{[M_{\tilde{d}}^{2(\text{diag})}]_{II}}{m_{\tilde{g}}^2}, \tag{2.4}$$

which we will use to express Wilson coefficients later on.

2.2 $\Delta B = 2$ effective Hamiltonian

For B_s - \overline{B}_s mixing, we use the $\Delta B = 2 (= -\Delta S)$ effective Hamiltonian. We first integrate out SUSY particles and derive effective Hamiltonian at sparticle mass scale. Then we use the renormalization group running formula from the sparticle mass scale to m_b scale presented in [22]. The resulting effective Hamiltonian can be written as

$$\mathcal{H}_{\text{eff}}^{\Delta B=2} = \sum_{i=1}^5 C_i Q_i + \sum_{i=1}^3 \tilde{C}_i \tilde{Q}_i + \text{h.c.}, \tag{2.5}$$

where we choose the operator basis as follows:

$$\begin{aligned} Q_1 &= \bar{s}_L^\alpha \gamma_\mu b_L^\alpha \bar{s}_L^\beta \gamma^\mu b_L^\beta, \\ Q_2 &= \bar{s}_R^\alpha b_L^\alpha \bar{s}_R^\beta b_L^\beta, \\ Q_3 &= \bar{s}_R^\alpha b_L^\beta \bar{s}_R^\beta b_L^\alpha, \\ Q_4 &= \bar{s}_R^\alpha b_L^\alpha \bar{s}_L^\beta b_R^\beta, \\ Q_5 &= \bar{s}_R^\alpha b_L^\beta \bar{s}_L^\beta b_R^\alpha, \end{aligned} \tag{2.6}$$

where α and β are color indices. The Wilson coefficients \mathcal{C}_i 's associated with the operator Q_i 's are given by

$$\begin{aligned}
\mathcal{C}_1 &= \frac{\alpha_s^2}{216m_{\tilde{g}}^2} \sum_{IJ} \Gamma_L^{I2*} \Gamma_L^{I3} \Gamma_L^{J2*} \Gamma_L^{J3} \left(-24B_2(r_I, r_J) - 264B_1(r_I, r_J) \right), \\
\mathcal{C}_2 &= \frac{\alpha_s^2}{216m_{\tilde{g}}^2} \sum_{IJ} \Gamma_R^{I2*} \Gamma_L^{I3} \Gamma_R^{J2*} \Gamma_L^{J3} \left(-204B_2(r_I, r_J) \right), \\
\mathcal{C}_3 &= \frac{\alpha_s^2}{216m_{\tilde{g}}^2} \sum_{IJ} \Gamma_R^{I2*} \Gamma_L^{I3} \Gamma_R^{J2*} \Gamma_L^{J3} \left(36B_2(r_I, r_J) \right), \\
\mathcal{C}_4 &= \frac{\alpha_s^2}{216m_{\tilde{g}}^2} \left[\sum_{IJ} \Gamma_R^{I2*} \Gamma_R^{I3} \Gamma_L^{J2*} \Gamma_L^{J3} \left(-504B_2(r_I, r_J) + 288B_1(r_I, r_J) \right) \right. \\
&\quad \left. + \sum_{IJ} \Gamma_L^{I2*} \Gamma_R^{I3} \Gamma_R^{J2*} \Gamma_L^{J3} \left(528B_1(r_I, r_J) \right) \right], \\
\mathcal{C}_5 &= \frac{\alpha_s^2}{216m_{\tilde{g}}^2} \left[\sum_{IJ} \Gamma_R^{I2*} \Gamma_R^{I3} \Gamma_L^{J2*} \Gamma_L^{J3} \left(-24B_2(r_I, r_J) - 480B_1(r_I, r_J) \right) \right. \\
&\quad \left. + \sum_{IJ} \Gamma_L^{I2*} \Gamma_R^{I3} \Gamma_R^{J2*} \Gamma_L^{J3} \left(720B_1(r_I, r_J) \right) \right],
\end{aligned} \tag{2.7}$$

where we use the notation

$$B_i(r_I, r_J) = \frac{B_i(r_I) - B_i(r_J)}{r_I - r_J}, \quad i = 1, 2, \tag{2.8}$$

with [23]

$$B_1(r) = -\frac{r^2 \ln r}{4(1-r)^2} - \frac{1}{4(1-r)}, \quad B_2(r) = -\frac{r \ln r}{(1-r)^2} - \frac{1}{1-r}. \tag{2.9}$$

One can get \tilde{O}_i and \tilde{C}_i for $i = 1, 2, 3$ by exchanging $L \leftrightarrow R$.

For the matrix elements of the above operators and the numerical values of $B_{1,\dots,5}(\mu)$ and f_{B_d} , we use the values given in Ref. [22]. We use the following ratio

$$\frac{f_{B_s} \sqrt{B_{B_s}}}{f_{B_d} \sqrt{B_{B_d}}} = 1.21, \tag{2.10}$$

given in Ref. [24].

2.3 $\Delta B = 1$ effective Hamiltonian

Nonleptonic charmless and radiative $B_{d(s)}$ decays are described by the following $\Delta B = 1$ effective Hamiltonian. We use the same normalization of operator basis as in Ref. [17]. RG running of gluino-loop contributions from m_W scale to m_b scale is performed in the way presented in [25], i.e., the α_s^n factor from the quark-squark-gluino vertices is included in an operator rather than the corresponding Wilson coefficient, and the dimension-five and dimension-six versions of the (chromo-)magnetic operators are treated separately. Then

the $\Delta B = 1$ effective Hamiltonian encoding the gluino-squark loop contribution can be written as

$$\mathcal{H}_{\text{eff}}^{\Delta B=1} = \frac{G_F}{\sqrt{2}} \sum_{p=u,c} \lambda_p \left[\sum_{i=3}^6 (C_i O_i + \tilde{C}_i \tilde{O}_i) + \sum_{i=7\gamma, 8g} (C_{ib} O_{ib} + C_{i\tilde{g}} O_{i\tilde{g}} + \tilde{C}_{ib} \tilde{O}_{ib} + \tilde{C}_{i\tilde{g}} \tilde{O}_{i\tilde{g}}) \right] + \text{h.c.}, \quad (2.11)$$

where $\lambda_p = V_{ps}^* V_{pb}$. The operator basis is chosen as follows:

$$\begin{aligned} O_3 &= \alpha_s^2 (\bar{s}b)_{V-A} \sum_q (\bar{q}q)_{V-A}, \\ O_4 &= \alpha_s^2 (\bar{s}_\alpha b_\beta)_{V-A} \sum_q (\bar{q}_\beta q_\alpha)_{V-A}, \\ O_5 &= \alpha_s^2 (\bar{s}b)_{V-A} \sum_q (\bar{q}q)_{V+A}, \\ O_6 &= \alpha_s^2 (\bar{s}_\alpha b_\beta)_{V-A} \sum_q (\bar{q}_\beta q_\alpha)_{V+A}, \\ O_{7\gamma b} &= -\frac{\alpha_s e}{8\pi^2} m_b \bar{s} \sigma_{\mu\nu} (1 + \gamma_5) F^{\mu\nu} b, \\ O_{8gb} &= -\frac{\alpha_s g_s}{8\pi^2} m_b \bar{s} \sigma_{\mu\nu} (1 + \gamma_5) G^{\mu\nu} b, \\ O_{7\gamma\tilde{g}} &= -\frac{\alpha_s e}{8\pi^2} \bar{s} \sigma_{\mu\nu} (1 + \gamma_5) F^{\mu\nu} b, \\ O_{8g\tilde{g}} &= -\frac{\alpha_s g_s}{8\pi^2} \bar{s} \sigma_{\mu\nu} (1 + \gamma_5) G^{\mu\nu} b. \end{aligned} \quad (2.12)$$

The corresponding Wilson coefficients C_i 's are given by

$$\begin{aligned}
C_3 &= -\frac{1}{2\sqrt{2}G_F m_{\tilde{g}}^2 \lambda_t} \left[\sum_I \Gamma_L^{I2*} \Gamma_L^{I3} \left(-\frac{1}{18} C_1(r_I) + \frac{1}{2} C_2(r_I) \right) \right. \\
&\quad \left. + \sum_{IJ} \Gamma_L^{I2*} \Gamma_L^{I3} \Gamma_L^{J2*} \Gamma_L^{J2} \left(-\frac{1}{9} B_1(r_I, r_J) - \frac{5}{9} B_2(r_I, r_J) \right) \right], \\
C_4 &= -\frac{1}{2\sqrt{2}G_F m_{\tilde{g}}^2 \lambda_t} \left[\sum_I \Gamma_L^{I2*} \Gamma_L^{I3} \left(\frac{1}{6} C_1(r_I) - \frac{3}{2} C_2(r_I) \right) \right. \\
&\quad \left. + \sum_{IJ} \Gamma_L^{I2*} \Gamma_L^{I3} \Gamma_L^{J2*} \Gamma_L^{J2} \left(-\frac{7}{3} B_1(r_I, r_J) + \frac{1}{3} B_2(r_I, r_J) \right) \right], \\
C_5 &= -\frac{1}{2\sqrt{2}G_F m_{\tilde{g}}^2 \lambda_t} \left[\sum_I \Gamma_L^{I2*} \Gamma_L^{I3} \left(-\frac{1}{18} C_1(r_I) + \frac{1}{2} C_2(r_I) \right) \right. \\
&\quad \left. + \sum_{IJ} \Gamma_L^{I2*} \Gamma_L^{I3} \Gamma_R^{J2*} \Gamma_R^{J2} \left(\frac{10}{9} B_1(r_I, r_J) + \frac{1}{18} B_2(r_I, r_J) \right) \right], \quad (2.13) \\
C_6 &= -\frac{1}{2\sqrt{2}G_F m_{\tilde{g}}^2 \lambda_t} \left[\sum_I \Gamma_L^{I2*} \Gamma_L^{I3} \left(\frac{1}{6} C_1(r_I) - \frac{3}{2} C_2(r_I) \right) \right. \\
&\quad \left. + \sum_{IJ} \Gamma_L^{I2*} \Gamma_L^{I3} \Gamma_R^{J2*} \Gamma_R^{J2} \left(-\frac{2}{3} B_1(r_I, r_J) + \frac{7}{6} B_2(r_I, r_J) \right) \right], \\
C_{7\gamma b} &= -\frac{\pi}{\sqrt{2}G_F m_{\tilde{g}}^2 \lambda_t} \sum_I \Gamma_L^{I2*} \Gamma_L^{I3} \left(-\frac{4}{9} D_1(r_I) \right), \\
C_{7\gamma \tilde{g}} &= -\frac{\pi}{\sqrt{2}G_F m_{\tilde{g}}^2 \lambda_t} \sum_I \Gamma_L^{I2*} \Gamma_R^{I3} \left(-\frac{4}{9} D_2(r_I) \right), \\
C_{8\gamma b} &= -\frac{\pi}{\sqrt{2}G_F m_{\tilde{g}}^2 \lambda_t} \sum_I \Gamma_L^{I2*} \Gamma_L^{I3} \left(-\frac{1}{6} D_1(r_I) + \frac{3}{2} D_3(r_I) \right), \\
C_{8\gamma \tilde{g}} &= -\frac{\pi}{\sqrt{2}G_F m_{\tilde{g}}^2 \lambda_t} \sum_I \Gamma_L^{I2*} \Gamma_R^{I3} \left(-\frac{1}{6} D_2(r_I) + \frac{3}{2} D_4(r_I) \right).
\end{aligned}$$

One can get \tilde{O}_i and \tilde{C}_i for $i = 3, \dots, 6, 7\gamma, 8g$ by exchanging $L \leftrightarrow R$. The loop functions

are given by Eqs. (2.8), (2.9), and [23]

$$\begin{aligned}
C_1(r) &= \frac{2r^3 - 9r^2 + 18r - 11 - 6 \ln r}{36(1-r)^4}, \\
C_2(r) &= \frac{-16r^3 + 45r^2 - 36r + 7 + 6r^2(2r-3) \ln r}{36(1-r)^4}, \\
D_1(r) &= \frac{-r^3 + 6r^2 - 3r - 2 - 6r \ln r}{6(1-r)^4}, \\
D_2(r) &= \frac{-r^2 + 1 + 2r \ln r}{(r-1)^3}, \\
D_3(r) &= \frac{2r^3 + 3r^2 - 6r + 1 - 6r^2 \ln r}{6(1-r)^4}, \\
D_4(r) &= \frac{-3r^2 + 4r - 1 + 2r^2 \ln r}{(r-1)^3}.
\end{aligned} \tag{2.14}$$

2.4 New elements in this analysis

SUSY effects in B_s mixing before the CDF/DØ measurements of ΔM_s have been discussed comprehensively in literatures [16, 17, 26]. This work is an update of our previous works [16, 17], including a few new elements and improvements in the analysis:

- We include the $\tan \beta$ dependent double mass insertion more carefully. As a result, the $B \rightarrow X_s \gamma$ branching ratio constrains not only the LR and RL insertions, but also the LL and RR insertions, because of the induced LR and RL mass insertions. Double mass insertion contribution to $B \rightarrow X_s \gamma$ has long been known [27]. Potential importance of the double mass insertion was discussed in Ref. [28] in the context of supersymmetric contributions to $\text{Re}(\epsilon'/\epsilon)$ using the $s \rightarrow dg$ operator, and similarly in Refs. [29, 30, 31] regarding $b \rightarrow s$ transitions. We discuss more on this in the next subsection in the context of $b \rightarrow s \gamma$ and $b \rightarrow sg$. Because of this improvement, we get stronger constraints on the pure LL or RR insertion, compared with our previous study [17], especially for large $\tan \beta$. (However, see also [32].)
- We also consider the simultaneous presence of the LL and RR insertions, motivated by some SUSY flavor models which predict $LL \approx RR$. We find that the ΔM_s measurement puts a stringent constraint on such cases, independent of $\tan \beta$ [27, 30, 31]. Our analysis shows that some SUSY flavor models are already excluded by (or marginally compatible with) the ΔM_s measurement of the CDF/DØ. Partly for simplicity, we consider only two cases where the two insertions are assumed to be correlated by $(\delta_{23}^d)_{LL} = \pm(\delta_{23}^d)_{RR}$. Regarding their phases, however, there are good reasons to restrict their difference around 0 or π . Sizeable LL and RR mass insertions with uncorrelated phases are likely to give an excessive contribution to the neutron EDM [33]. For instance, if $\mu = 500$ GeV and the sizes of the two insertions are both around 0.05 (see Figs.6–9 (a)), then the neutron EDM limits their relative phase within $\lesssim 0.8/\tan \beta$ around 0 or π .

- We include the $D\bar{O}/CDF$ data on the phase of B_s mixing deduced from the dilepton charge asymmetry and $B_s \rightarrow J/\psi\phi$ [14, 15, 34]. In particular, we discuss consequences of the present tendency of the data favoring a negative $O(1)$ value of ϕ_s [35].
- We present the time dependent CP asymmetry in $B^0 \rightarrow K^{*0}\gamma$, in cases with right-handed $b \leftrightarrow s$ currents such as from the RR insertion. See Ref. [36] for more details on this observable.
- In this paper, we consider only the LL and RR insertions, and do not consider LR or RL insertion, because the new data on ΔM_s does not affect the analysis in Ref. [16, 17] on LR or RL insertion. In that article, we have found that the $B \rightarrow X_s\gamma$ constraint on these chirality-flipping insertions is so strong that they cannot give an appreciable modification to ΔM_s or ϕ_s [17, 26].

2.5 Double mass insertion

If the LL or RR insertion is sizable and $\mu \tan \beta$ is large, the effective LR or RL insertion can be induced due to the double mass insertion mechanism we discussed in the previous subsection and in Refs. [27, 28, 29]. Then we can expect that $B \rightarrow X_s\gamma$ could give a strong constraint on the LL or RR insertion through this effective LR or RL insertion. The relevant Feynman diagram is shown in Fig. 1. The induced LR or RL from double mass insertion can be written schematically as

$$(\delta_{LR}^d)_{23}^{\text{ind}} = (\delta_{LL}^d)_{23} \times \frac{m_b(A_b - \mu \tan \beta)}{\tilde{m}^2}. \quad (2.15)$$

Therefore, we have

$$(\delta_{LL,RR}^d)_{23} \sim 10^{-2} \rightarrow (\delta_{LR,RL}^d)_{23}^{\text{ind}} \sim 10^{-2},$$

if $\mu \tan \beta \sim 30 \text{ TeV}$. This can be expected if $\tan \beta$ is large ~ 40 . For larger LL, RR mixing, even smaller $\mu \tan \beta$ would suffice to induce the LR, RL mass insertions of a size $10^{-2} - 10^{-3}$. Since $\delta_{LL,RR}^d$'s in SUSY flavor models are generically complex, the induced $(\delta_{LR}^d)_{23}^{\text{ind}}$ could carry a new CP violating phase even if the trilinear coupling A_b and μ parameters are real. In such a case, there could be strong correlations among various CP violating observables. The effects of these induced LR or RL mixing appear in the deviations in $S_{CP}^{\phi K}$, $A_{CP}^{b \rightarrow s\gamma}$, or $S_{CP}^{K^*\gamma}$ from their SM predictions.

It is important to remember that the effect of the induced LR insertion is different from that of the single LR insertion, since they involve different numbers of squark propagators in the relevant Feynman diagrams, and thus yielding different loop functions when one evaluates the Feynman diagrams.

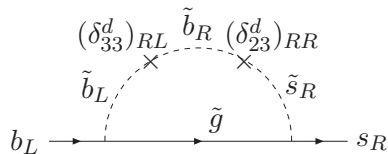


Figure 1: Gluino-squark loop graph with double mass insertion for $B \rightarrow X_s\gamma$.

2.6 Numerical analysis

In the following discussions and numerical analysis, we fix the SUSY parameters as follows once and for all:

$$m_{\tilde{q}} = m_{\tilde{g}} = \mu = 500 \text{ GeV},$$

$$\tan\beta = 3 \text{ and } 10,$$

taking the mass insertion parameters $(\delta_{23}^d)_{AB}$'s as a free complex parameter. We do not consider very high $\tan\beta \gtrsim 30$ at which double Higgs penguin contribution may be important [10, 37]. Since we do not include the chargino contributions in this work, the sign of μ could be either positive or negative. However, we choose a positive μ , since it is preferred by the muon $g-2$ when we include the chargino or the neutralino contributions. The plots for a negative μ are similar to those for a positive μ . If the supersymmetric contribution to an observable is dominated by double mass insertion, the region allowed by it is almost reflected around zero. The small difference arises from interference between single and double insertions. Such observables include $B(B \rightarrow X_s\gamma)$, $A_{CP}^{b \rightarrow s\gamma}$, $S_{CP}^{\phi K}$, and $S_{CP}^{K^*\gamma}$. Therefore, the compatibility of each case with these observables discussed later largely remains the same even if we take the negative sign of μ . When we scan over the complex parameter $(\delta_{23}^d)_{AB}$'s, we impose the following constraints and show the excluded regions:

- Smallest squared mass eigenvalue in M_d^2 is required to be greater than $(100 \text{ GeV})^2$. The region incompatible with this requirement is denoted by gray hatched regions.
- The branching ratio of $B \rightarrow X_s\gamma$ is required to be within its 2σ range [6],

$$3.0 \times 10^{-4} < B(B \rightarrow X_s\gamma) < 4.1 \times 10^{-4}. \quad (2.16)$$

The region incompatible with this requirement is denoted by hatched regions.

- The region allowed by $12.4 \text{ ps}^{-1} < \Delta M_s < 23.1 \text{ ps}^{-1}$ is denoted by cyan regions. We allow for up to 30% of deviation of ΔM_s from the CDF central value [3], considering uncertainties in lattice QCD calculation and the CKM matrix elements (see e.g. [38] and references therein).
- The region allowed by both the ΔM_s constraint and $\phi_s \in [-1.10, -0.36] \cup [-2.77, -2.07]$ [35], where ϕ_s is $\arg(M_{12})$, is denoted by blue regions. We take the latest 95% probability range of ϕ_s . We adopt the sign of ϕ_s used in Refs. [39, 40].
- Then we predict the time dependent CP asymmetry ($S_{CP}^{\phi K}$) in $B_d \rightarrow \phi K_S$, that ($S_{CP}^{K^*\gamma}$) in $B^0 \rightarrow K^{*0}\gamma$, and the direct CP asymmetry ($A_{CP}^{b \rightarrow s\gamma}$) in $B \rightarrow X_s\gamma$.
- A black square denotes the SM prediction for each observable.
- We show the region corresponding to the 2σ range of $S_{CP}^{\phi K}$ in the plots for the allowed regions in the $(\text{Re}\delta, \text{Im}\delta)$ plane, using the current average $S_{CP}^{\phi K} = 0.39 \pm 0.18$ [6]. For this, we take into account the uncertainty in the prediction of $S_{CP}^{\phi K}$ coming from the

annihilation contribution in QCD factorization [41] in the same way as in Section VI.E of Ref. [17]. That is, the prediction of $S_{CP}^{\phi K}$ from a single point of δ forms an interval. We exclude the point of δ if the interval is mutually exclusive with the 2σ range from experiments. We use this interval in a correlation plot as well.

3. SUSY effects in $b \rightarrow s$ after the CDF/DØ measurements of ΔM_s

3.1 LL insertion case

Let us first consider the LL insertion (or LL dominance) case with $\tan\beta = 3$. In the previous study [16, 17], we ignored the double mass insertion so that the constraint on the LL insertion was not very strong. In this work, we include the induced LR insertion which is dependent on $\tan\beta$. Therefore, the $B \rightarrow X_s\gamma$ branching ratio puts a strong constraint, even before we impose the ΔM_s measurements. Only the unhatched region is consistent with $B \rightarrow X_s\gamma$ constraint in Fig. 2 (a). A substantial part of $(\delta_{23}^d)_{LL}$ is already excluded by $B \rightarrow X_s\gamma$. After imposing the CDF/DØ data on ΔM_s and ϕ_s , only the blue region remains allowed. It is outstanding that the SM point lies outside the blue region indicating that the current ϕ_s data, with the aid of ΔM_s , is pointing to a new source of flavor/ CP violation. Moreover, the size of insertion needed to fit the B_s mixing data is of $O(1)$. This large insertion inevitably disturbs $B \rightarrow X_s\gamma$ through the double mass insertion mechanism involving the $\mu \tan\beta$ term. Indeed, one finds that most of the blue region is ruled out by the branching ratio of $B \rightarrow X_s\gamma$. Note that $B \rightarrow X_s\gamma$ is this stringent already with $\tan\beta$ as low as 3 and that it grows tighter as $\tan\beta$ increases as we will see shortly. Still, there are corners compatible with $B \rightarrow X_s\gamma$ as well as $B_s-\overline{B}_s$ mixing, which is evident from Fig. (b). The plot also shows that one of the two ϕ_s solutions is excluded by $B \rightarrow X_s\gamma$. The double insertion leads to sizable changes in $S_{CP}^{\phi K}$ or $A_{CP}^{b \rightarrow s\gamma}$ as well. Fig. (c) shows that $B \rightarrow X_s\gamma$ and $B_s-\overline{B}_s$ mixing, together, disfavor $S_{CP}^{\phi K}$ around its SM value, although it is still permitted to fall within its 2σ range. The same set of constraints results in $A_{CP}^{b \rightarrow s\gamma}$ of \pm a few per cent, as displayed in Fig. (d), which can be discriminated from the SM prediction at a super B factory.

For $\tan\beta = 10$, the double mass insertion becomes more important, and $(\delta_{23}^d)_{LL}$ is strongly constrained by $B \rightarrow X_s\gamma$ and B_s mixing constraints. The results are shown in Figs. 3. The allowed region of $(\delta_{23}^d)_{LL}$ is the narrow unhatched blue strip in Fig. (a). Comparing Figs. 3 (b) and 2 (b), one also finds that the phase of $B_s-\overline{B}_s$ mixing is more tightly constrained compared to the previous case with $\tan\beta = 3$. Also, $S_{CP}^{\phi K}$ and $A_{CP}^{b \rightarrow s\gamma}$ can deviate from their SM values significantly through the induced LR insertion. Fig. 3 (a) reveals that the narrow strip allowed by B_s mixing and $B \rightarrow X_s\gamma$ leads to $S_{CP}^{\phi K}$ out of its 2σ range. In this sense, this case with large LL insertion and moderately high $\tan\beta$ is disfavored by the current B physics data. The predicted range of $S_{CP}^{\phi K}$ is found to be higher than its SM value, around 0.9, in Fig. (c). In Fig. (d), we find that the blue unhatched region corresponds to $A_{CP}^{b \rightarrow s\gamma}$ around negative several per cent.

3.2 RR insertion case

Next, we consider the RR insertion case for $\tan\beta = 3, 10$, which are shown in Figs. 4–5. The

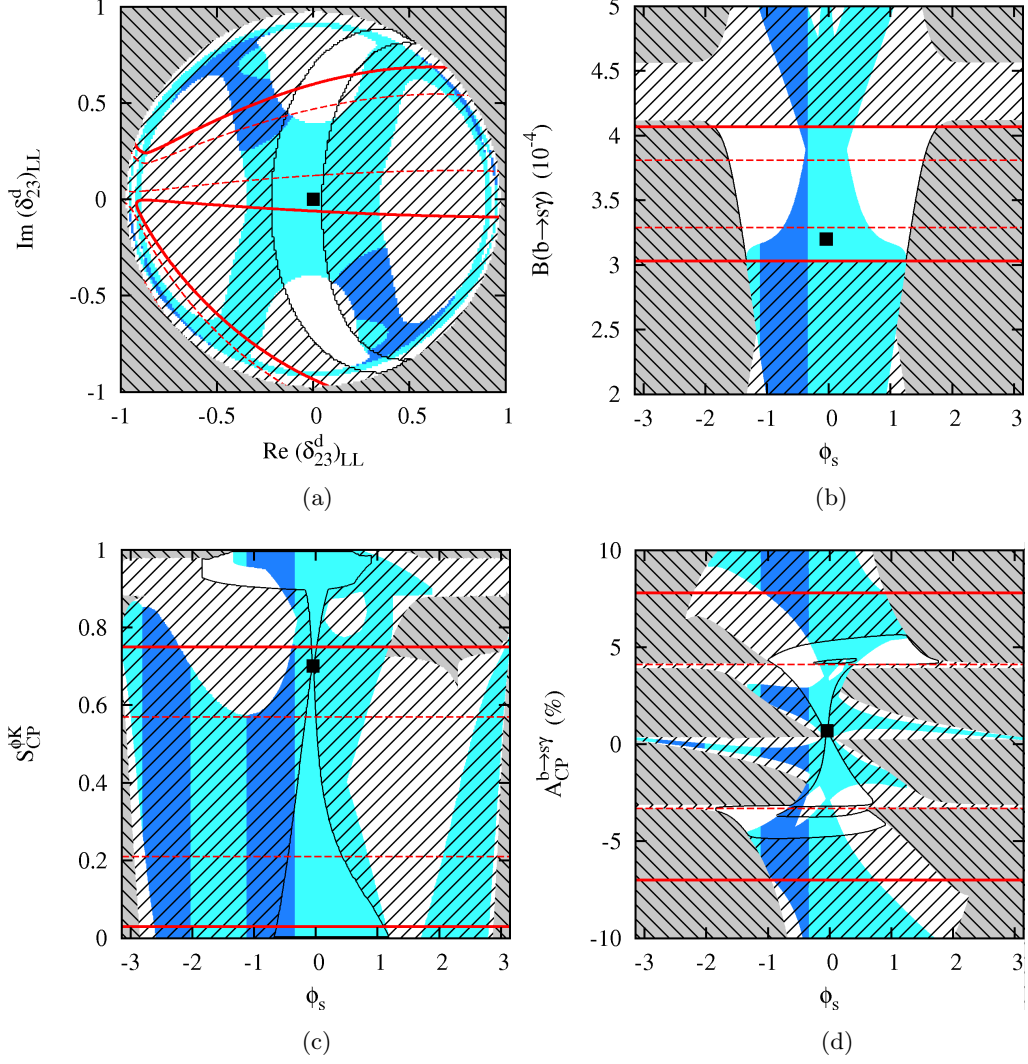


Figure 2: The LL insertion case with $\tan\beta = 3$. Allowed regions on (a) $(\text{Re}(\delta_{23}^d)_{LL}, \text{Im}(\delta_{23}^d)_{LL})$, and correlation between ϕ_s and each of (b) $B(B \rightarrow X_s\gamma)$, (c) $S_{CP}^{\phi_K}$, and (d) $A_{CP}^{b \rightarrow s\gamma}$. The hatched gray region leads to the lightest squark mass < 100 GeV. The hatched region is excluded by the $B \rightarrow X_s\gamma$ constraint. The cyan region is allowed by ΔM_s . The blue region is allowed both by ΔM_s and ϕ_s . The black square is the SM point. In Fig. (a), bands bounded by red dashed and solid curves correspond to 1σ and 2σ ranges of S_{ϕ_K} , respectively. In the rest figures, red dashed and solid lines mark 1σ and 2σ ranges of each observable, respectively.

shapes of the allowed regions, after the $B \rightarrow X_s\gamma$ constraint is imposed, are different from those in the LL insertion case, since there is no interference between the SUSY amplitude (the original RR or the induced RL type) and the SM amplitude (LR type). However, the general tendency is similar to the LL insertion case: namely, the induced RL insertion involving the double mass insertion is constrained by the $B \rightarrow X_s\gamma$ branching ratio, and the constraint becomes severer for larger $\tan\beta$.

In Fig. 4, the ΔM_s and ϕ_s constraints again excludes the origin and requires nonzero squark mixing depicted by the blue region. We observe that $B \rightarrow X_s\gamma$ leaves a broader

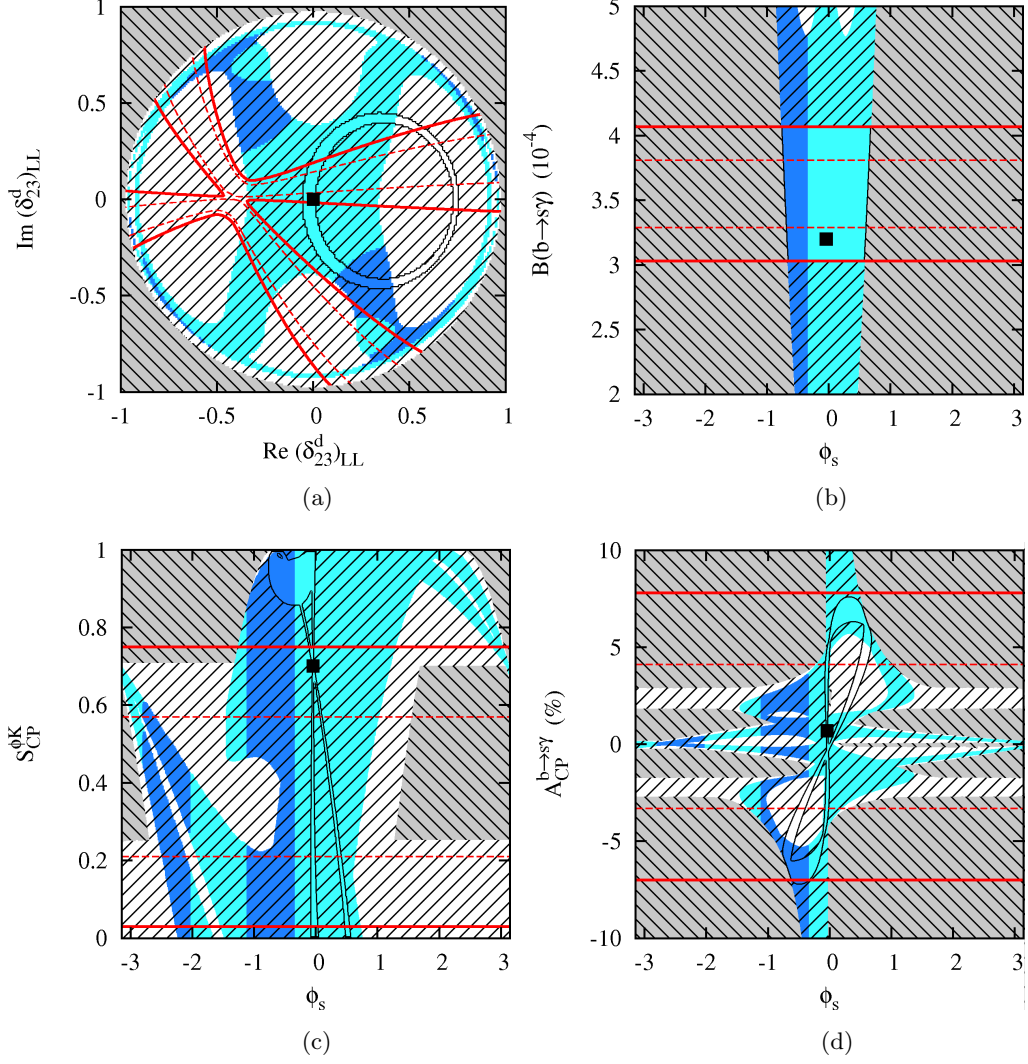


Figure 3: Plots with the LL insertion for $\tan\beta = 10$. The meaning of each region is the same as in Figs. 2.

region than in the LL case (compare Figs. 4 (a) and 2 (a)). In particular, there remains a larger portion of unhatched blue region, due to the weaker constraint from $B \rightarrow X_s\gamma$. Still, only one of the two solutions of ϕ_s is allowed in Fig. 4 (b). The induced RL insertion can lead to sizable changes in $S_{CP}^{\phi K}$ and/or $S_{CP}^{K^*\gamma}$ as well, as shown in Figs. (c) and (d). Each of them deviates from its SM value due to the $O(1)$ phase of $(\delta_{23}^d)_{RR}$ favored by ϕ_s , under the $B \rightarrow X_s\gamma$ constraint. Although $S_{CP}^{\phi K}$ is expelled from the SM point, it can still remain consistent with its measurements. Note that $S_{CP}^{K^*\gamma}$ could be as large as around ± 0.8 , and these values are in fact preferred by ϕ_s and $B \rightarrow X_s\gamma$. This would be clearly tested at B factories.

For $\tan\beta = 10$, the double mass insertion becomes more important, and $(\delta_{23}^d)_{RR}$ is strongly constrained by both $B \rightarrow X_s\gamma$ and B_s mixing. The results are shown in Fig. 5 (a). In this case, the region of $(\delta_{23}^d)_{RR}$ allowed by $B \rightarrow X_s\gamma$ and ΔM_s is smaller

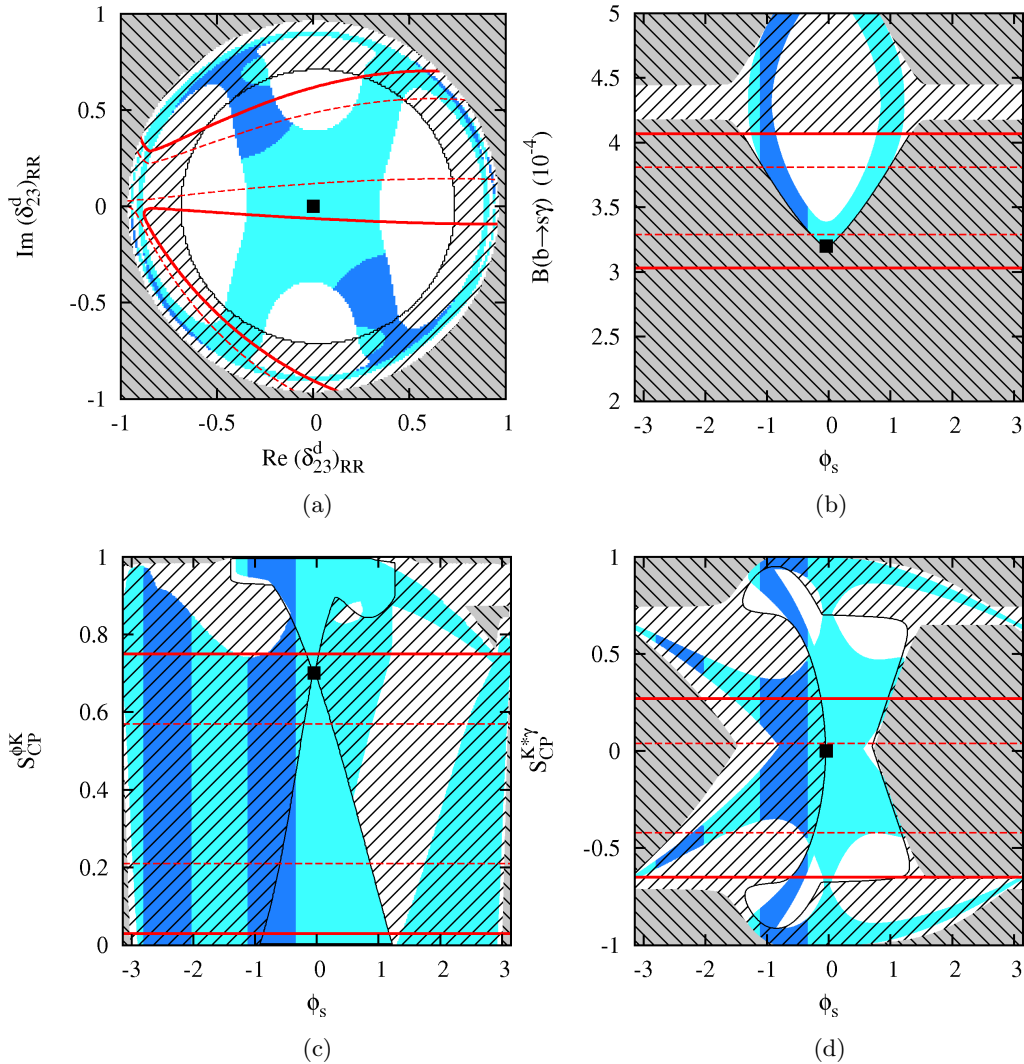


Figure 4: The RR insertion case with $\tan\beta = 3$. The meaning of each region is the same as in Figs. 2.

than the previous case with $\tan\beta = 3$. Moreover, the limitation is so strong that the measured value of ϕ_s cannot be reached. Therefore, this case with large RR insertion and moderately high $\tan\beta$ is disfavored by the current B physics data. Indeed, ϕ_s is confined within a narrow range around the SM value and thus no unhatched blue region can be found in Fig. (b). Forgetting about the current status of ϕ_s , one might estimate effects of the RR insertion within the unhatched cyan region on $S_{CP}^{\phi K}$ and $A_{CP}^{b\rightarrow s\gamma}$. They may deviate from their SM values significantly through induced RL insertion, as shown in Figs. (c) and (d).

3.3 $LL = RR$ case

In this section, we consider the $LL = RR$ case with $\tan\beta = 3, 10$, which are shown in Figs. 6 and 7, respectively. In this case, the supersymmetric effect on $B_s-\overline{B}_s$ mixing is

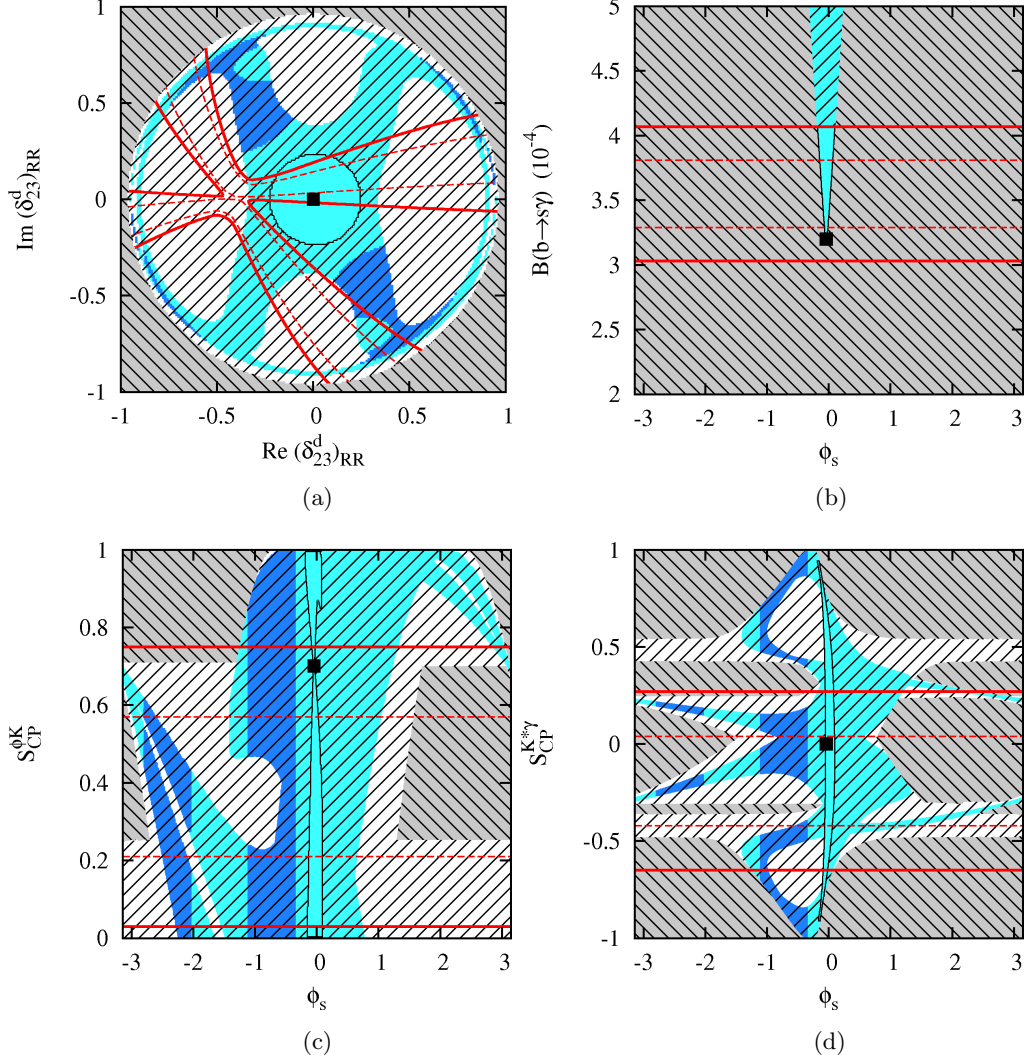


Figure 5: Plots with the RR insertion for $\tan\beta = 10$. The meaning of each region is the same as in Figs. 2.

greatly enhanced compared to the LL or the RR insertion case, while that on $B \rightarrow X_s\gamma$ is not. Thus, only a tiny region around zero is allowed even for small $\tan\beta = 3$, shown in Fig. 6 (a). The phase of the mixing is not constrained significantly by $B \rightarrow X_s\gamma$, and this decay alone allows for an arbitrary ϕ_s , as can be seen in the other three plots. These plots also show variations in $S_{CP}^{K^*\gamma}$, $S_{CP}^{\phi K}$, and $A_{CP}^{b \rightarrow s\gamma}$, but they are much smaller than are found in the preceding cases with a single insertion of either chirality, since ΔM_s allows a much smaller squark mixing. This means that this case can account for the current data of ϕ_s as well as ΔM_s while obeying the other constraints on CP asymmetries under consideration. Still, differences of $S_{CP}^{K^*\gamma}$ and $S_{CP}^{\phi K}$ from their SM predictions can be comparable to or larger than their sensitivities at a super B factory, while $A_{CP}^{b \rightarrow s\gamma}$ is not altered enough. Note that the blue region again implies a non-vanishing discrepancy in $S_{CP}^{\phi K}$.

The results for a higher $\tan\beta = 10$ are shown in Fig. 7. The $B \rightarrow X_s\gamma$ constraint

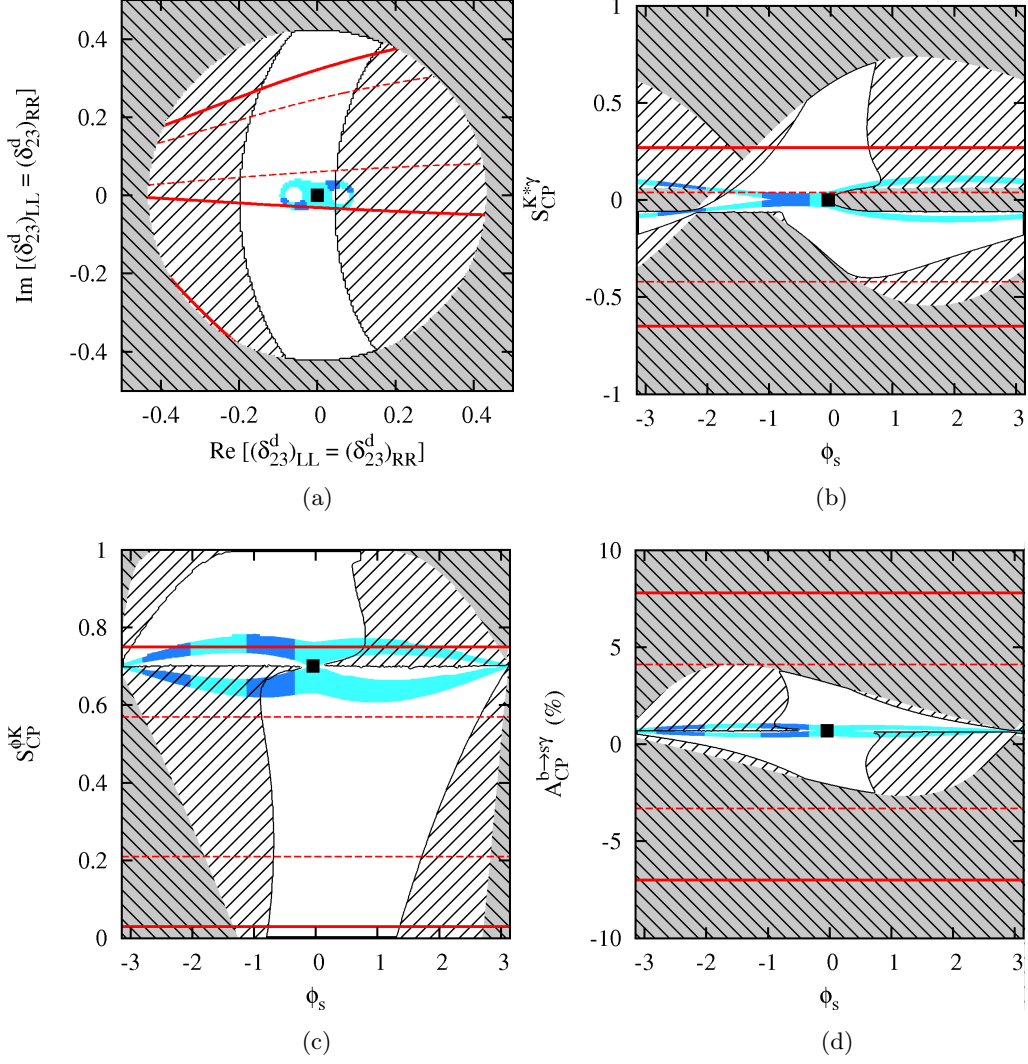


Figure 6: Plots for the $LL = RR$ case with $\tan\beta = 3$. The meaning of each region is the same as in Figs. 2.

becomes stronger. Because of this, the range of ϕ_s is reduced, but it can still be consistent with the present data. Also, the increased effect of the double insertion leads to larger deviations in $S_{CP}^{K^*\gamma}$, $S_{CP}^{\phi K}$, and $A_{CP}^{b\rightarrow s\gamma}$. In particular, one finds that the unhatched blue region leading to $S_{CP}^{\phi K} \sim 0.9$ is excluded from its 2σ band in Fig. (c). Therefore this case is disfavored by the current data. Note that the SUSY effect in $S_{CP}^{\phi K}$ depends on the sum of the LL and RR (or LR and RL) insertions, and this makes a clear difference between the predictions of CP asymmetry in this case and the next.

3.4 $LL = -RR$ case

In this section, we consider the $LL = -RR$ case. The results for $\tan\beta = 3$ are shown in Figs. 8. Note that the $B_s - \bar{B}_s$ mixing constraint is again much stronger than a case with a single insertion of either chirality, and only a tiny region around zero is allowed. The

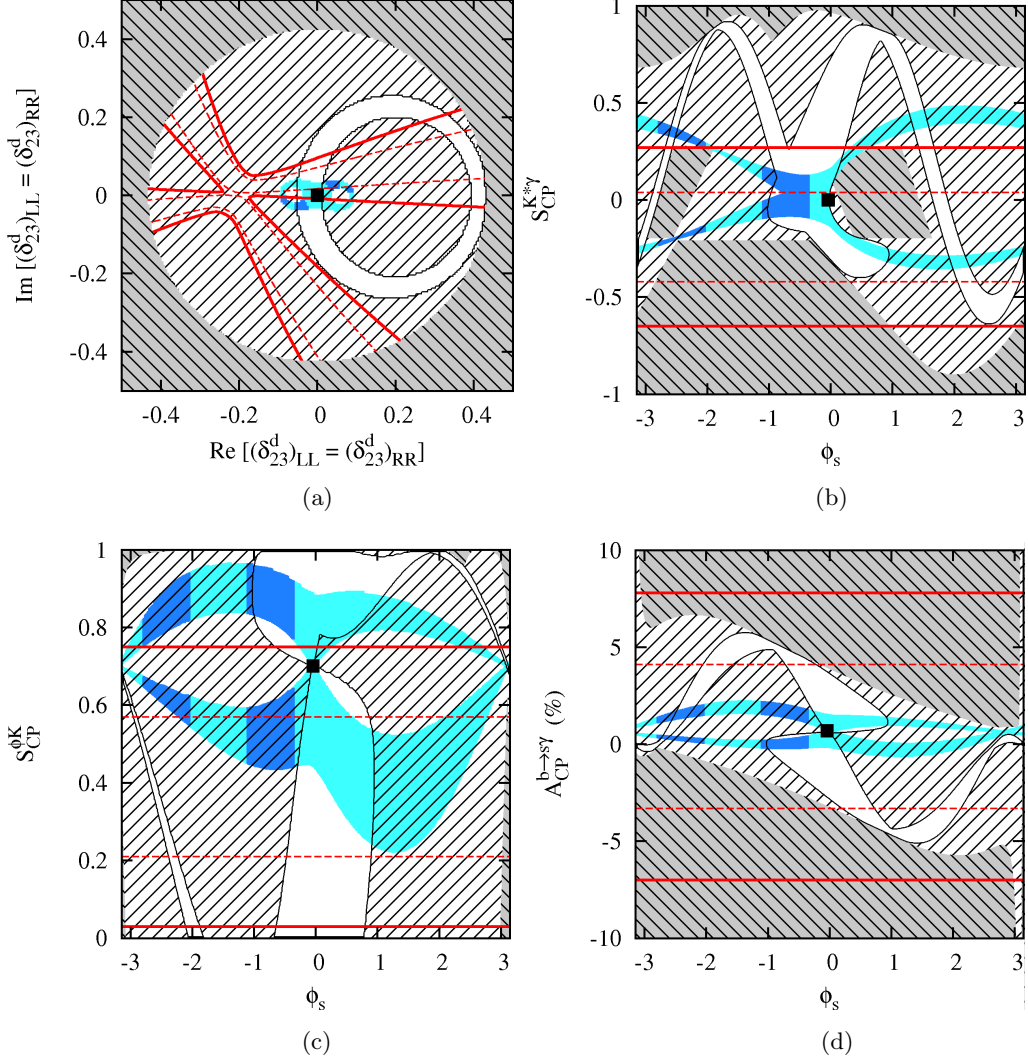


Figure 7: Plots for the $LL = RR$ case with $\tan\beta = 10$. The meaning of each region is the same as in Figs. 2.

phase of the mixing can be arbitrary even after $B \rightarrow X_s\gamma$ has been imposed, as is shown in Fig. (b). The deviation in $S_{CP}^{K^*\gamma}$ can be comparable to or larger than its sensitivities at a super B factory, while $A_{CP}^{b \rightarrow s\gamma}$ is not altered enough. In this case, $S_{CP}^{\phi K}$ does not move from its SM value, as the SUSY effect in $S_{CP}^{\phi K}$ depends on the sum of the LL and RR (or LR and RL) insertions which cancel each other. Therefore $S_{CP}^{\phi K}$ is not affected even for higher $\tan\beta$. Instead, $S_{CP}^{\eta K}$ should show a discrepancy as it depends on the difference of the LL and RR (or LR and RL) insertions.

Results for a higher $\tan\beta = 10$ are shown in Figs. 9. The $B \rightarrow X_s\gamma$ constraint becomes stronger. Nevertheless, ϕ_s is allowed to have an arbitrary value. Deviations in $S_{CP}^{K^*\gamma}$ and $A_{CP}^{b \rightarrow s\gamma}$ has been amplified relative to the previous case with $\tan\beta = 5$. As was mentioned above, $S_{CP}^{\phi K}$ remains at its SM prediction. This helps the present case to be compatible with all of the experimental inputs, $B \rightarrow X_s\gamma$, ΔM_s , ϕ_s , and $S_{CP}^{\phi K}$, even for a moderately

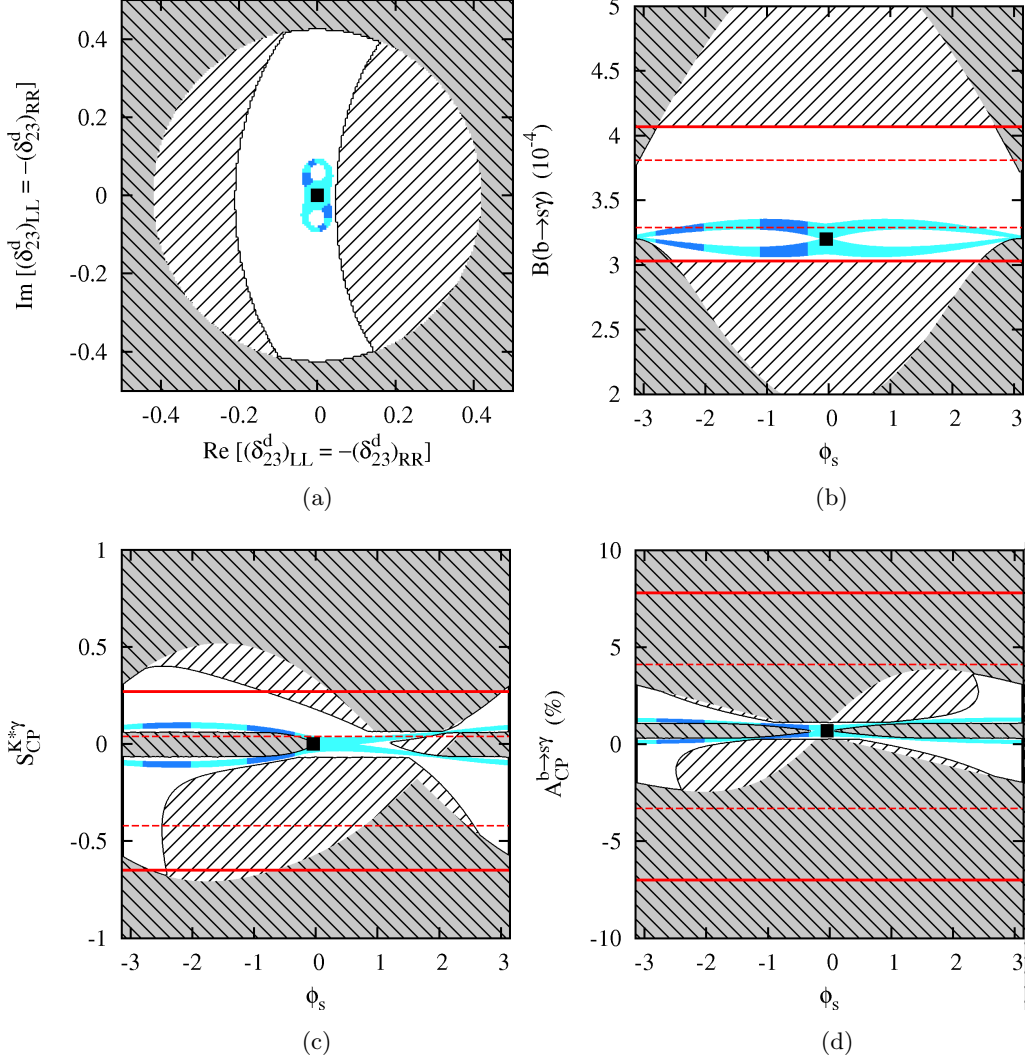


Figure 8: Plots for the $LL = -RR$ case with $\tan\beta = 3$. The meaning of each region is the same as in Figs. 2.

high $\tan\beta$. Recall that the $LL = RR$ case, by contrast, was in conflict with $S_{CP}^{\phi K}$ for the same value of $\tan\beta$. The phase of mass insertions in the unhatched blue region causes non-vanishing deviations in $S_{CP}^{K^*\gamma}$ and $A_{CP}^{b\rightarrow s\gamma}$, to such an extent that can be tested at a B factory.

3.5 Implications for $B_s \rightarrow \mu^+\mu^-$

In the previous sections, we derived the constraints on the LL and RR insertions related to the 23 mixing in the squark sector. Gluino mediated flavor violation of $b \rightarrow s$ can affect another rare B_s decay, $B_s \rightarrow \mu^+\mu^-$. Isidori and Retico obtained bounds on $\delta_{LL,RR}$'s from

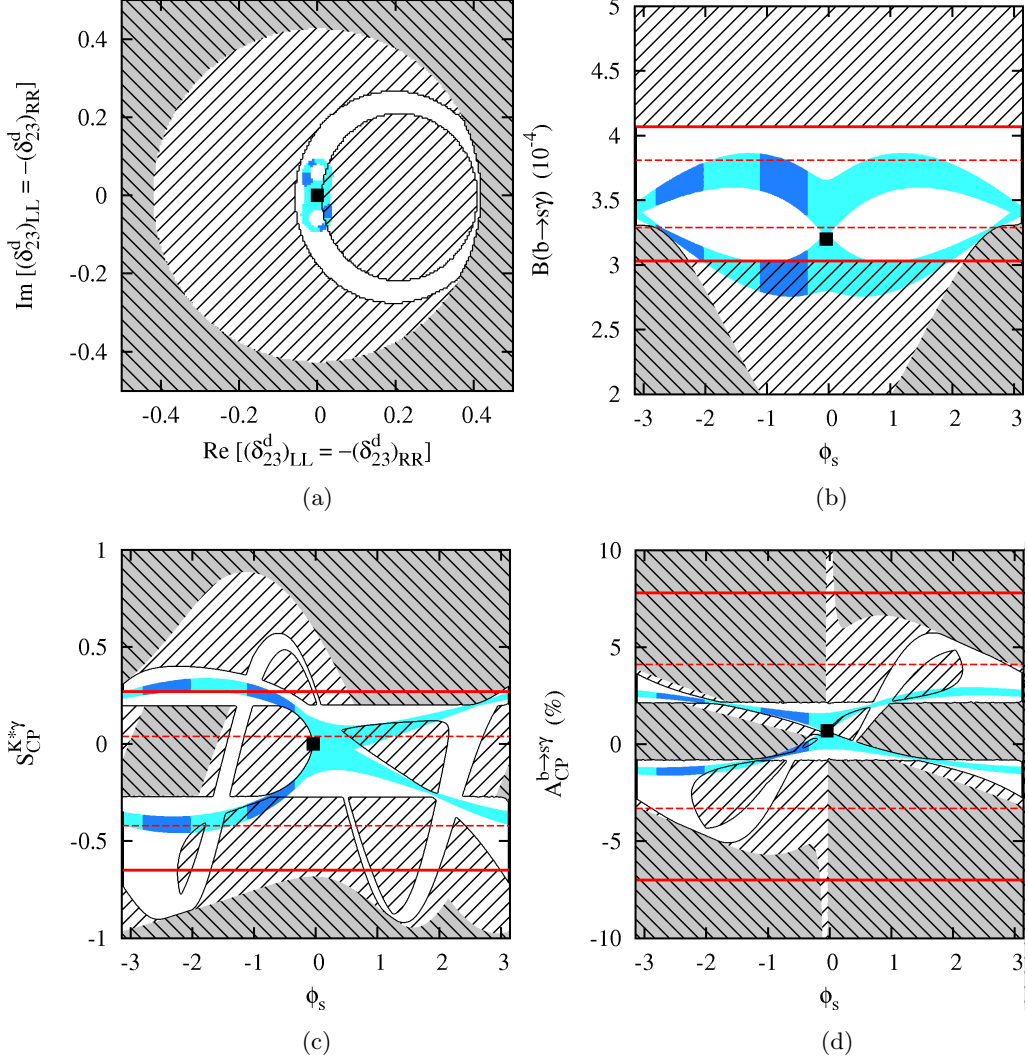


Figure 9: Plots for the $LL = -RR$ case with $\tan\beta = 10$. The meaning of each region is the same as in Figs. 2

$B(B_s \rightarrow \mu^+\mu^-)$ for light $m_A \approx 200$ GeV and large $\tan\beta$ [42]:

$$\frac{B(B_s \rightarrow \mu^+\mu^-)}{B_{\text{SM}}(B_s \rightarrow \mu^+\mu^-)} \approx 1.5 \times 10^5 \left(\frac{200}{M_A(\text{GeV})} \right)^4 |(\delta_{23}^d)_{LL,RR}|^2 \frac{\left(\frac{\tan\beta}{50} \right)^6}{\left[\frac{2}{3} + \frac{1}{3} \left(\frac{\tan\beta}{50} \right) \right]^4} \quad (3.1)$$

Our constraint is independent of m_A , and is mainly driven by $B \rightarrow X_s\gamma$ for large $\tan\beta$ case, where $B_s \rightarrow \mu^+\mu^-$ can be enhanced.

Note that $|\delta_{LL,RR}^d| \lesssim 0.05$ for $\tan\beta = 40$ from $B_s - \bar{B}_s$ mixing. This constraint and the ones considered in the preceding sections are complementary with each other. For small and moderate $\tan\beta \lesssim 30$, the constraint derived in this work from $B \rightarrow X_s\gamma$ and ΔM_s is more important than that from $B_s \rightarrow \mu^+\mu^-$.

The gluino contributions to $B_s \rightarrow \mu^+\mu^-$ is not that important in general, unless m_A is light and $\tan\beta$ is very large.

4. Implications for SUSY models

In Sec. 3, we derived the constraint on $(\delta_{23}^d)_{LL}$ and $(\delta_{23}^d)_{RR}$. The size of δ 's are determined by theories for the soft SUSY breaking, or SUSY breaking mediation mechanisms. There are basically three categories in the solutions to the SUSY flavor and CP problems:

- Universal scalar masses at some messenger scale
- Alignment of quark and squark mass matrices in the flavor space using some flavor symmetry
- Decoupling (effective SUSY scenario).

In this section, we discuss implications of the analysis in the previous section on the flavor structures of the soft terms at high energy scale and on SUSY flavor models, for the first two categories listed above to which our results are applicable.

4.1 SUSY models with universal scalar masses

Let us first discuss the flavor physics within SUSY scenarios where one has universal soft terms at some high energy messenger scale M_{mess} . In this case, the SUSY flavor problem is solved by assuming universal squark mass matrices at M_{mess} . Nonetheless at electroweak scale, non-vanishing mass insertion parameters are generated by RG evolution, which is calculable in terms of the Yukawa couplings. Namely, $\delta_{ij}(M_{\text{mess}}) = 0$, and nonzero δ 's at the electroweak scale are generated by RG evolutions. Models belonging to this category include the so-called minimal supergravity (mSUGRA) or gauge mediation SUSY breaking scenarios, dilaton dominated SUSY breaking within superstring models.

For example, within mSUGRA, one has [43]

$$(\Delta_{ij})_{LL}(M_Z) \simeq -\frac{1}{8\pi^2} Y_t^2 (V_{\text{CKM}})_{3i} (V_{\text{CKM}}^*)_{3j} (3m_0^2 + a_0^2) \log\left(\frac{M_*}{M_Z}\right), \quad (4.1)$$

so that $(\delta_{LL}^d)_{23} \simeq 10^{-2}$ and $(\delta_{LL}^d)_{13} \simeq 8 \times 10^{-3} \times e^{-i2.7}$. This size of $(\delta_{23}^d)_{LL}$ might be regarded as being perfectly fine with the constraints we discussed in Subsection 3.1, unless one cares about the current status of ϕ_s . If one is interested in fitting the present data of ϕ_s , this scenario is not a good choice. In particular, the phase of $(\delta_{23}^d)_{LL}$ is -0.02 . Therefore, there would be only small deviations in ϕ_s , $S_{CP}^{\phi K}$, or $A_{CP}^{b \rightarrow s \gamma}$ within this scenario. There could be some effects in $b \rightarrow d$ transition, including $B \rightarrow X_d \gamma$, and we refer to Ref. [19] for further details.

If we consider a SUSY grand unified theory (GUT) with right handed neutrinos, the situation can change, however. In many SUSY GUT models, the left handed lepton doublet sits in the same representation as the left-handed anti-down quark triplets. Then, the large mixing in the atmospheric neutrinos could be related with the large mixing in the $\tilde{b}_R - \tilde{s}_R$ sector [23, 44, 45], unless the main source of neutrino mixings is the Majorana right-handed neutrino mass terms. Therefore there could be large $b \rightarrow s$ transitions in the low energy processes in such scenarios, and B_s mixing or $B_d \rightarrow \phi K_S$ CP asymmetries can differ significantly from the SM predictions.

For example, in SU(5) with right-handed neutrinos, one has [23, 44]

$$\begin{aligned} (m_{\tilde{d}}^2)_{ij} &\simeq -\frac{1}{8\pi^2} [Y_N^\dagger Y_N]_{ij} (3m_0^2 + A^2) \log \frac{M_*}{M_{\text{GUT}}} \\ &\simeq -e^{-i(\phi_i^{(L)} - \phi_j^{(L)})} \frac{y_{\nu_k}^2}{8\pi^2} [V_L^*]_{ki} [V_L]_{kj} (3m_0^2 + A^2) \log \frac{M_*}{M_{\text{GUT}}}. \end{aligned}$$

In this scenario, $|(\delta_{RR}^d)_{23}| \simeq 2 \times 10^{-2} \times (M_{N_3}/10^{14} \text{ GeV})$ with $O(1)$ phase, which is in sharp contrast with the LL insertion, Eq. (4.1). This RG induced δ alone is small enough to evade the constraint from ΔM_s , but not big enough to accommodate ϕ_s . On the other hand, the RR insertion is large enough to induce an effective RL insertion of $\sim 10^{-2}$ through the double mass insertion mechanism, and can affect $S_{CP}^{\phi K}$ and $S_{CP}^{K^*\gamma}$. Also in this scenario, there are RG induced LL insertions mentioned above. Combining these two types of insertions, one could get enough effect in $B_s - \bar{B}_s$ mixing to fit the current world average of ϕ_s . However, an obstacle to this purpose is hadronic electric dipole moment [46]. In particular, it is not easy to circumvent this constraint if one assumes that the LL insertion arises solely from RG evolution, as is the case in this subsection. One of the few ways might be to assume that the first and the second terms in $A_b - \mu \tan\beta$ cancel each other resulting in a small sum, since the supersymmetric contribution to hadronic electric dipole moment is proportional to the sum.

4.2 SUSY flavor models

Another way out of the SUSY flavor problem is to invoke some flavor symmetry and make quark and squark mass matrices almost aligned. Alignment of quark and squark mass matrices can be achieved by assuming some flavour symmetries ($U(1), S_3, \dots$). We discuss what implications the present analysis may have on those supersymmetric flavor models. We borrow the list of models from Ref. [47], discarding two decoupling type models therein.

Suppose that a given flavor symmetry is broken around the GUT scale. Then RG evolution of the squark mass matrix down to the weak scale should be taken into account. The diagonal components increase receiving the gluino mass contribution:

$$m_{\tilde{q}}^2(M_Z) \approx m_0^2 + 6 M_{1/2}^2, \quad (4.2)$$

where m_0 and $M_{1/2}$ are the diagonal squark mass and the gluino mass at the GUT scale. An off-diagonal element does not change very much except for the CKM suppressed contribution in Eq. (4.1). In many cases, a flavor symmetry predicts the ratio of an off-diagonal element to the diagonal one, $(\Delta_{ij})_{AB}/m_0^2$, thereby determining the degree of squark non-universality at the scale where it is broken. In terms of this ratio, the mass insertion at weak scale can be written as

$$(\delta_{ij}^d)_{AB} \approx \frac{(\Delta_{ij})_{AB}/m_0^2}{1 + 6 M_{1/2}^2/m_0^2}, \quad (4.3)$$

using Eq. (4.2). One can notice that the non-universality at the GUT scale is diluted in the course of running, depending on the ratio $M_{1/2}^2/m_0^2$. In what follows, we ignore this

effect. If one takes it into account, constraints on a model may be eased especially for large $M_{1/2}$. On the other hand, this could also make it more difficult to account for the present $O(1)$ value of ϕ_s by reducing the expected size of a mass insertion below what is needed.

The result is shown in Table 1. The current status of each model is indicated in the

Model	$ (\delta_{23}^d)_{LL} $	$ (\delta_{23}^d)_{RR} $	$\tan\beta = 3$	$\tan\beta = 10$
[48]	λ^2	λ^4	\cdot	\checkmark
[49], [50]a	λ^2	1	\times	\times
[51]	λ^2	λ^8	\cdot	\checkmark
[50]b	λ^2	$\lambda^{1/2}$	\times	\times
[52], [53]b	λ^2	λ^2	ϕ_s	\checkmark
[54]	λ^3	λ^5	\cdot	\cdot
[55]	λ^2	λ^4	\cdot	\checkmark

Table 1: Status of part of the models analyzed in Ref. [47], for the two different values of $\tan\beta$. Each case is classified into one of the following four categories: (\cdot) incompatible with ϕ_s but safe otherwise; (ϕ_s) compatible with ϕ_s and safe; (\checkmark) currently okay but dangerous; (\times) disfavored.

two columns on the right. One can see that availability of the new data on $B_s - \overline{B}_s$ mixing enables us to discriminate models according to their predictions on 2–3 mixing of down-type squarks. A Model is marked as being safe if it suppresses flavor violation to such an extent that no appreciable deviation from the SM can be observed. However, such a model may not produce enough difference in ϕ_s to account for its current world average. We indicate a class of models that can fit ϕ_s while keeping compatibility with the other constraints. They lead to nonzero mass insertions of both chiralities enhancing supersymmetric contribution to B_s mixing. A caveat is dilution of mass insertions mentioned above. Some models leading to sizeable mass insertions are about to be in contact with the present experiments or strongly disfavored by them depending on the choice of parameters. A future experiment should be able to resolve this issue and to scrutinize more models. Needless to say, all the above discussions are based on our choice of sparticle mass scale. That is, supersymmetric flavor/ CP problems can be mitigated by making sparticles heavier.

5. Conclusions

In conclusions, we studied the implication of the recent measurements of $B_s - \overline{B}_s$ mixing on the mass insertion parameters in the general SUSY models and on the SUSY flavor models. The recent measurements of ΔM_s constrains the CKM element $|V_{td}|$, which is consistent with the Belle result extracted from $b \rightarrow d\gamma$. This constitutes another test of the CKM paradigm of the SM for flavor and CP violation in the quark sector. The measurement of ΔM_s begins to put strong constraint on new physics scenarios, and a room for the new physics contribution to $b \rightarrow s$ transition is getting tight now, and will be even more so in the future. Even the very first data on ΔM_s from DØ and CDF already constrain either of the LL and the RR insertions, which should be compared with the bounds $\lesssim O(1)$ in [17] or [26]. For the $LL = \pm RR$ case, the constraints are even stronger, and the allowed mass

insertion parameters are tiny even for small $\tan\beta = 3$. Still there could be moderate to large deviations in $A_{CP}^{b\rightarrow s\gamma}$, $S_{CP}^{K^*\gamma}$, or $S_{CP}^{\phi K}$ through the double mass insertion effects for large $\tan\beta$ case. It is imperative to measure these observables, and confirm the SM predictions on these observables both at hadron colliders and at (super) B factories, in order to test the CKM paradigm in the $b \rightarrow s$ transition.

In a model independent approach, one can say that CP violation in $B_s \rightarrow J/\psi\phi$ and A_{SL} give additional informations on the phase of $B_s-\overline{B}_s$ mixing, and can make a firm test of the CKM paradigm in the SM, and constrain various new physics scenarios. CP asymmetries in $B \rightarrow \phi K_S, \eta' K_S, K_S\pi^0, \dots$ can differ from the SM predictions to some extent, but we cannot make definite predictions within the model independent approach.

Within general SUSY models with gluino mediated $b \rightarrow s$ transition, one can summarize the implications of the ΔM_s and ϕ_s measurements as follows:

- The LL or RR insertions for small $\tan\beta$ case cannot be large as in the past ($\lesssim 0.5$)
- Large $\tan\beta$ case is strongly constrained by $b \rightarrow s\gamma$ (independent of m_A) and by $B_s \rightarrow \mu^+\mu^-$ for light m_A
- The $LL = \pm RR$ case is even more strongly constrained by ΔM_s measurement
- The LR or RL insertions consistent with $b \rightarrow s\gamma$ is still fine with ΔM_s , since it does not affect $B_s-\overline{B}_s$ mixing; however for the same reason, it cannot make an $O(1)$ difference in ϕ_s
- Definite relations between $\Delta B = 2$ and $\Delta B = 1$ processes CP asymmetries in $B \rightarrow \phi K_S, \eta' K_S, K_S\pi^0, \dots$ can differ from the SM predictions to some extent, and we can make definite predictions within SUSY models (modulo hadronic uncertainties)
- $B_d \rightarrow \phi K_S$ can still differ from the SM prediction, if the (induced) LR or RL insertions are present at the level of $10^{-2}-10^{-3}$

Whether the present hint of new physics in B_s mixing phase will persist in the future or not will be an interesting topic within coming years for B factories and hadron colliders, and the data will show whether the SM explains $b \rightarrow s$ transition perfectly, or some new physics is in need. In particular it is important to improve the precision of time dependent CP asymmetries in $B_s \rightarrow J/\psi\phi$ and $B_d \rightarrow \phi K_S$, and the direct CP asymmetry in $B \rightarrow X_s\gamma$ *etc.*, and confront the measured data with the SM predictions, in order to confirm the Kobayashi-Maskawa paradigm or discover indirect new physics effects.

Acknowledgments

We are grateful to Intae Yu for discussions on the experimental data from DØ and CDF. PK is supported in part by KOSEF through the SRC program at CHEP, Kyungpook National University. JhP acknowledges Research Grants funded jointly by the Italian Ministero dell'Istruzione, dell'Università e della Ricerca (MIUR), by the University of Padova

and by the Istituto Nazionale di Fisica Nucleare (INFN) within the *Astroparticle Physics Project* and the FA51 INFN Research Project. He was also supported in part by the European Community Research Training Network UniverseNet under contract MRTN-CT-2006-035863.

References

- [1] N. Cabibbo, *Unitary Symmetry and Leptonic Decays*, *Phys. Rev. Lett.* **10** (1963) 531; M. Kobayashi and T. Maskawa, *CP violation in the renormalizable theory of weak interaction*, *Prog. Theor. Phys.* **49** (1973) 652.
- [2] V. M. Abazov *et al.* [DØ Collaboration], *Direct Limits on the B_s^0 Oscillation Frequency*, *Phys. Rev. Lett.* **97** (2006) 021802 [[hep-ex/0603029](#)].
- [3] A. Abulencia *et al.* [CDF Collaboration], *Observation of $B_s^0-\overline{B}_s^0$ oscillations*, *Phys. Rev. Lett.* **97** (2006) 242003 [[hep-ex/0609040](#)].
- [4] K. Abe *et al.*, *Observation of $b \rightarrow d\gamma$ and determination of $|V_{td}/V_{ts}|$* , *Phys. Rev. Lett.* **96** (2006) 221601 [[hep-ex/0506079](#)].
- [5] J. Charles *et al.* [CKMfitter Group], *CP violation and the CKM matrix: Assessing the impact of the asymmetric B factories*, *Eur. Phys. J.* **C41** (2005) 1 [[hep-ph/0406184](#)]; updated results and plots available at: <http://ckmfitter.in2p3.fr/>
- [6] E. Barberio *et al.*, *Averages of b-hadron and c-hadron Properties at the End of 2007*, [arXiv:0808.1297](#) [hep-ex].
- [7] Y. Grossman, Y. Nir and G. Raz, *Constraining the phase of B/s - anti-B/s mixing*, *Phys. Rev. Lett.* **97** (2006) 151801 [[hep-ph/0605028](#)].
- [8] A. Lenz and U. Nierste, *Theoretical update of B/s - anti-B/s mixing*, *JHEP* **0706** (2007) 072 [[hep-ph/0612167](#)].
- [9] M. Ciuchini and L. Silvestrini, *Upper bounds on SUSY contributions to $b \rightarrow s$ transitions from $B_s-\overline{B}_s$ mixing*, *Phys. Rev. Lett.* **97** (2006) 021803 [[hep-ph/0603114](#)]; M. Endo and S. Mishima, *Constraint on right-handed squark mixings from $B_s-\overline{B}_s$ mass difference*, *Phys. Lett.* **B640** (2006) 205 [[hep-ph/0603251](#)]; P. Ball and R. Fleischer, *Probing new physics through B mixing: Status, benchmarks and prospects*, *Eur. Phys. J.* **C48** (2006) 413 [[hep-ph/0604249](#)]; S. Khalil, *Supersymmetric contribution to the CP asymmetry of $B \rightarrow J/\psi\phi$ in the light of recent $B_s-\overline{B}_s$ measurements*, *Phys. Rev.* **D74** (2006) 035005 [[hep-ph/0605021](#)]; S. Baek, *$B_s-\overline{B}_s$ mixing in the MSSM scenario with large flavor mixing in the LL/RR sector*, *JHEP* **0609** (2006) 077 [[hep-ph/0605182](#)]; R. Arnowitt, B. Dutta, B. Hu and S. Oh, *$B_s-\overline{B}_s$ mixing and its implication for $b \rightarrow s$ transitions in supersymmetry*, *Phys. Lett.* **B641** (2006) 305 [[hep-ph/0606130](#)]; B. Dutta and Y. Mimura, *$B_s-\overline{B}_s$ mixing in grand unified models*, *Phys. Rev. Lett.* **97** (2006) 241802 [[hep-ph/0607147](#)]; X. Ji, Y. Li and Y. Zhang, *Atmospheric neutrino mixing and $b \rightarrow s$ transitions: Testing lopsided $SO(10)$ flavor structure in B physics*, *Phys. Rev.* **D75** (2007) 055016 [[hep-ph/0612114](#)].
- [10] J. Foster, K. i. Okumura and L. Roszkowski, *New constraints on SUSY flavour mixing in light of recent measurements at the Tevatron*, *Phys. Lett.* **B641** (2006) 452 [[hep-ph/0604121](#)].

- [11] A. Datta, B_s mixing and new physics in hadronic $b \rightarrow s\bar{q}q$ transitions, *Phys. Rev.* **D74** (2006) 014022 [[hep-ph/0605039](#)]; X. G. He and G. Valencia, $B_s-\bar{B}_s$ mixing constraints on FCNC and a non-universal Z' , *Phys. Rev.* **D74** (2006) 013011 [[hep-ph/0605202](#)]; M. Blanke, A. J. Buras, A. Poschenrieder, C. Tarantino, S. Uhlig and A. Weiler, Particle-antiparticle mixing, ϵ_K , $\Delta\Gamma_q$, A_{SL}^q , $A_{CP}(B_d \rightarrow \psi K_S)$, $A_{CP}(B_s \rightarrow \psi\phi)$ and $B \rightarrow X_{s,d}\gamma$ in the Littlest Higgs model with T -parity, *JHEP* **0612** (2006) 003 [[hep-ph/0605214](#)]; C. W. Chiang, N. G. Deshpande and J. Jiang, Flavor changing effects in family nonuniversal Z' models, *JHEP* **0608** (2006) 075 [[hep-ph/0606122](#)]; S. Baek, J. H. Jeon and C. S. Kim, $B_s^0-\bar{B}_s^0$ mixing in leptophobic Z' model, *Phys. Lett. B* **641** (2006) 183 [[hep-ph/0607113](#)]; A. J. Buras, A. Poschenrieder, S. Uhlig and W. A. Bardeen, Rare K and B decays in the littlest Higgs model without T -parity, *JHEP* **0611** (2006) 062 [[hep-ph/0607189](#)]; S. Chang, C. S. Kim and J. Song, Constraint of $B_{d,s}^0-\bar{B}_{d,s}^0$ mixing on warped extra-dimension model, *JHEP* **0702** (2007) 087 [[hep-ph/0607313](#)]; L. x. Lu and Z. j. Xiao, $B_{s(d)}^0-\bar{B}_{s(d)}^0$ mixing and new physics effects in a top quark two-Higgs doublet model, *Commun. Theor. Phys.* **47** (2007) 1099 [[hep-ph/0609279](#)]; A. Dighe, A. Kundu and S. Nandi, Possibility of large lifetime differences in neutral B meson systems, *Phys. Rev. D* **76** (2007) 054005 [[arXiv:0705.4547](#) [hep-ph]]; R. Mohanta and A. K. Giri, Unparticle effect on $B_s-\bar{B}_s$ mixing and its implications for $B_s \rightarrow J/\psi\phi$, $\phi\phi$ decays, *Phys. Rev. D* **76** (2007) 075015 [[arXiv:0707.1234](#) [hep-ph]]; A. Lenz, Unparticle physics effects in B_s mixing, *Phys. Rev. D* **76** (2007) 065006 [[arXiv:0707.1535](#) [hep-ph]]; S. L. Chen, X. G. He, X. Q. Li, H. C. Tsai and Z. T. Wei, Constraints on Unparticle Interactions from Particle and Antiparticle Oscillations, [arXiv:0710.3663](#) [hep-ph]; J. P. Lee and K. Young Lee, Implications of the anomalous top quark couplings in $B_s-\bar{B}_s$ mixing, $B \rightarrow X_s\gamma$ and top quark decays, [arXiv:0806.1389](#) [hep-ph].
- [12] For a review, see e.g. Y. Nir, *CP violation in meson decays*, [hep-ph/0510413](#).
- [13] For a review, see e.g. R. Fleischer, *Flavour Physics and CP Violation: Expecting the LHC*, [arXiv:0802.2882](#) [hep-ph].
- [14] V. M. Abazov *et al.* [DØ Collaboration], Measurement of B_s^0 mixing parameters from the flavor-tagged decay, [arXiv:0802.2255](#) [hep-ex].
- [15] T. Aaltonen *et al.* [CDF Collaboration], First Flavor-Tagged Determination of Bounds on Mixing-Induced CP Violation in $B_s \rightarrow J/\psi\phi$ Decays, *Phys. Rev. Lett.* **100** (2008) 161802 [[arXiv:0712.2397](#) [hep-ex]].
- [16] G. L. Kane, P. Ko, H. b. Wang, C. Kolda, J.-h. Park and L. T. Wang, $B_d \rightarrow \phi K_S$ CP asymmetries as an important probe of supersymmetry, *Phys. Rev. Lett.* **90** (2003) 141803 [[hep-ph/0304239](#)];
- [17] $B_d \rightarrow \phi K_S$ and supersymmetry, *Phys. Rev.* **D70** (2004) 035015 [[hep-ph/0212092](#)].
- [18] For a review, see e.g. S. P. Martin, *A supersymmetry primer*, [hep-ph/9709356](#).
- [19] P. Ko, J.-h. Park and G. Kramer, $B^0-\bar{B}^0$ mixing, $B \rightarrow J/\psi K_S$ and $B \rightarrow X_d\gamma$ in general MSSM, *Eur. Phys. J.* **C25** (2002) 615 [[hep-ph/0206297](#)].
- [20] L. J. Hall, V. A. Kostelecky and S. Raby, New flavor violations in supergravity models, *Nucl. Phys.* **B267** (1986) 415.
- [21] S. Baek, D. G. Cerdeno, Y. G. Kim, P. Ko and C. Munoz, Direct detection of neutralino dark matter in supergravity, *JHEP* **0506** (2005) 017 [[hep-ph/0505019](#)].
- [22] D. Becirevic *et al.*, $B_d-\bar{B}_d$ mixing and the $B_d \rightarrow J/\psi K_S$ asymmetry in general SUSY models, *Nucl. Phys.* **B634** (2002) 105 [[hep-ph/0112303](#)].

- [23] T. Moroi, *CP violation in $B_d \rightarrow \phi K_S$ in SUSY GUT with right-handed neutrinos*, *Phys. Lett.* **B493** (2000) 366 [[hep-ph/0007328](#)].
- [24] M. Okamoto, *Full determination of the CKM matrix using recent results from lattice QCD*, *PoS LAT2005* (2006) 013 [[hep-lat/0510113](#)].
- [25] F. Borzumati, C. Greub, T. Hurth and D. Wyler, *Gluino contribution to radiative B decays: Organization of QCD corrections and leading order results*, *Phys. Rev.* **D62** (2000) 075005 [[hep-ph/9911245](#)].
- [26] M. Ciuchini, E. Franco, A. Masiero and L. Silvestrini, *$b \rightarrow s$ transitions: A new frontier for indirect SUSY searches*, *Phys. Rev.* **D67** (2003) 075016 [Erratum-ibid. **D68** (2003) 079901] [[hep-ph/0212397](#)].
- [27] F. Gabbiani and A. Masiero, *FCNC in generalized supersymmetric theories*, *Nucl. Phys.* **B322** (1989) 235.
- [28] S. Baek, J. H. Jang, P. Ko and J.-h. Park, *Fully supersymmetric CP violations in the kaon system*, *Phys. Rev.* **D62** (2000) 117701 [[hep-ph/9907572](#)]; *Gluino-squark contributions to CP violations in the kaon system*, *Nucl. Phys.* **B609** (2001) 442 [[hep-ph/0105028](#)].
- [29] R. Harnik, D. T. Larson, H. Murayama and A. Pierce, *Atmospheric neutrinos can make beauty strange*, *Phys. Rev.* **D69** (2004) 094024 [[hep-ph/0212180](#)]; M. Endo, S. Mishima and M. Yamaguchi, *Recent measurements of CP asymmetries of $B \rightarrow \phi K^0$ and $B \rightarrow \eta' K_S$ at B-factories suggest new CP violation in left-handed squark mixing*, *Phys. Lett.* **B609** (2005) 95 [[hep-ph/0409245](#)].
- [30] M. Ciuchini and L. Silvestrini, *Upper bounds on SUSY contributions to $b \rightarrow s$ transitions from $B_s - \overline{B}_s$ mixing*, *Phys. Rev. Lett.* **97** (2006) 021803 [[hep-ph/0603114](#)].
- [31] M. Endo and S. Mishima, *Constraint on right-handed squark mixings from $B_s - \overline{B}_s$ mass difference*, *Phys. Lett.* **B640** (2006) 205 [[hep-ph/0603251](#)].
- [32] K. i. Okumura and L. Roszkowski, *Weakened Constraints from $b \rightarrow s\gamma$ on Supersymmetry Flavor Mixing Due to Next-To-Leading-Order Corrections*, *Phys. Rev. Lett.* **92** (2004) 161801 [[hep-ph/0208101](#)]; K. i. Okumura and L. Roszkowski, *Large beyond-leading-order effects in $b \rightarrow s\gamma$ in supersymmetry with general flavor mixing*, *JHEP* **0310** (2003) 024 [[hep-ph/0308102](#)].
- [33] J. Hisano and Y. Shimizu, *Hadronic EDMs induced by the strangeness and constraints on supersymmetric CP phases*, *Phys. Rev.* **D70** (2004) 093001 [[hep-ph/0406091](#)]; J. Hisano, M. Kakizaki, M. Nagai and Y. Shimizu, *Hadronic EDMs in SUSY SU(5) GUTs with right-handed neutrinos*, *Phys. Lett.* **B604** (2004) 216 [[hep-ph/0407169](#)].
- [34] V. M. Abazov *et al.* [DØ Collaboration], *Measurement of the charge asymmetry in semileptonic B_s^0 decays*, *Phys. Rev. Lett.* **98** (2007) 151801 [[hep-ex/0701007](#)]; *Lifetime difference and CP-violating phase in the B_s^0 system*, *Phys. Rev. Lett.* **98** (2007) 121801 [[hep-ex/0701012](#)]; V. M. Abazov *et al.* [DØ Collaboration], *Combined DØ measurements constraining the CP-violating phase and width difference in the B_s^0 system*, *Phys. Rev. D* **76** (2007) 057101 [[hep-ex/0702030](#)].
- [35] M. Bona *et al.* [UTfit Collaboration], *First evidence of new physics in $b \leftrightarrow s$ transitions*, [arXiv:0803.0659](#) [hep-ph].
- [36] D. Atwood, M. Gronau and A. Soni, *Mixing-induced CP asymmetries in radiative B decays in and beyond the standard model*, *Phys. Rev. Lett.* **79** (1997) 185 [[hep-ph/9704272](#)].

- [37] A. Dedes and A. Pilaftsis, *Resummed effective Lagrangian for Higgs-mediated FCNC interactions in the CP-violating MSSM*, *Phys. Rev.* **D67** (2003) 015012 [[hep-ph/0209306](#)]; M. S. Carena, A. Menon, R. Noriega-Papaqui, A. Szykman and C. E. M. Wagner, *Constraints on B and Higgs physics in minimal low energy supersymmetric models*, *Phys. Rev.* **D74** (2006) 015009 [[hep-ph/0603106](#)]; M. Blanke, A. J. Buras, D. Guadagnoli and C. Tarantino, *Minimal Flavour Violation Waiting for Precise Measurements of ΔM_s , $S_{\psi\phi}$, A_{SL}^s , $|V_{ub}|$, γ and $B_{s,d}^0 \rightarrow \mu^+\mu^-$* , *JHEP* **0610** (2006) 003 [[hep-ph/0604057](#)]; G. Isidori and P. Paradisi, *Hints of large $\tan\beta$ in flavour physics*, *Phys. Lett.* **B639** (2006) 499 [[hep-ph/0605012](#)].
- [38] A. Lenz and U. Nierste, *Theoretical update of B_s - \overline{B}_s mixing*, *JHEP* **0706** (2007) 072 [[hep-ph/0612167](#)].
- [39] V. M. Abazov *et al.* [DØ Collaboration], *Combined DØ measurements constraining the CP-violating phase and width difference in the B_s^0 system*, *Phys. Rev.* **D76** (2007) 057101 [[hep-ex/0702030](#)].
- [40] I. Dunietz, R. Fleischer and U. Nierste, *In pursuit of new physics with B_s decays*, *Phys. Rev.* **D63** (2001) 114015 [[hep-ph/0012219](#)].
- [41] M. Beneke, G. Buchalla, M. Neubert and C. T. Sachrajda, *QCD factorization for $B \rightarrow \pi\pi$ decays: Strong phases and CP violation in the heavy quark limit*, *Phys. Rev. Lett.* **83** (1999) 1914 [[hep-ph/9905312](#)]; *QCD factorization for exclusive, non-leptonic B-meson decays: General arguments and the case of heavy-light final states*, *Nucl. Phys.* **B591** (2000) 313 [[hep-ph/0006124](#)]; *QCD factorization in $B \rightarrow \pi K, \pi\pi$ decays and extraction of Wolfenstein parameters*, *Nucl. Phys.* **B606** (2001) 245 [[hep-ph/0104110](#)].
- [42] G. Isidori and A. Retico, *$B_{s,d} \rightarrow l^+l^-$ and $K_L \rightarrow l^+l^-$ in SUSY models with non-minimal sources of flavour mixing*, *JHEP* **0209** (2002) 063 [[hep-ph/0208159](#)].
- [43] L. Alvarez-Gaume, M. Claudson and M. B. Wise, *Low-energy supersymmetry*, *Nucl. Phys.* **B207** (1982) 96.
- [44] T. Moroi, *Effects of the right-handed neutrinos on $\Delta S = 2$ and $\Delta B = 2$ processes in supersymmetric SU(5) model*, *JHEP* **0003** (2000) 019 [[hep-ph/0002208](#)].
- [45] D. Chang, A. Masiero and H. Murayama, *Neutrino mixing and large CP violation in B physics*, *Phys. Rev.* **D67** (2003) 075013 [[hep-ph/0205111](#)].
- [46] Pyungwon Ko, Jae-hyeon Park and Masahiro Yamaguchi, in preparation.
- [47] L. Randall and S. f. Su, *CP violating lepton asymmetries from B decays and their implication for Nucl. Phys.* **B540** (1999) 37 [[hep-ph/9807377](#)].
- [48] M. Leurer, Y. Nir and N. Seiberg, *Mass matrix models: The Sequel*, *Nucl. Phys.* **B420** (1994) 468 [[hep-ph/9310320](#)].
- [49] Y. Nir and N. Seiberg, *Should squarks be degenerate?*, *Phys. Lett.* **B309** (1993) 337 [[hep-ph/9304307](#)].
- [50] C. D. Carone, L. J. Hall and T. Moroi, *New mechanism of flavor symmetry breaking from supersymmetric strong dynamics*, *Phys. Rev.* **D56** (1997) 7183 [[hep-ph/9705383](#)].
- [51] Y. Nir and R. Rattazzi, *Solving the Supersymmetric CP Problem with Abelian Horizontal Symmetries*, *Phys. Lett.* **B382** (1996) 363 [[hep-ph/9603233](#)].

- [52] R. Barbieri, L. J. Hall, S. Raby and A. Romanino, *Unified theories with $U(2)$ flavor symmetry*, *Nucl. Phys.* **B493** (1997) 3 [[hep-ph/9610449](#)].
- [53] A. Pomarol and D. Tommasini, *Horizontal symmetries for the supersymmetric flavor problem*, *Nucl. Phys.* **B466** (1996) 3 [[hep-ph/9507462](#)].
- [54] L. J. Hall and H. Murayama, *A geometry of the generations*, *Phys. Rev. Lett.* **75** (1995) 3985 [[hep-ph/9508296](#)]; C. D. Carone, L. J. Hall and H. Murayama, *$(S_3)^3$ flavor symmetry and $p \rightarrow K^0 e^+$* , *Phys. Rev.* **D53** (1996) 6282 [[hep-ph/9512399](#)].
- [55] P. Pouliot and N. Seiberg, *(S) quark masses and non-Abelian horizontal symmetries*, *Phys. Lett.* **B318** (1993) 169 [[hep-ph/9308363](#)].